Analysis of the Partially Filled
Viscous Ring Damper

Kyle T. Alfriend
Cornell University

Final Report NASA GRANT NGR-33-010-169
October 1973

Abstract

A ring partially filled with a viscous fluid has been analyzed as a nutation damper for a spinning satellite. The fluid has been modelled as a rigid slug of finite length moving in a tube and resisted by a linear viscous force. It is shown that there are two distinct modes of motion, called the spin synchronous mode and the nutation synchronous mode. Time constants for each mode are obtained for both the symmetric and asymmetric satellite. The effects of a stop in the tube and an offset of the ring from the spin axis are also investigated. An analysis of test results is also given including a determination of the effect of gravity on the time constants in the two modes.

Contents

Illustrations

Symbols

A, B,	- transverse moments of inertia of the satellite
C	- spin axis moment of inertia of the satellite
$\underset{\sim}{H}$	- angular momentum vector with components H_u, H_v, H_z
H_t	- transverse angular momentum
$I^*_{\alpha\beta}$	- moments and products of inertia of the fluid slug
R	- radius of the annulus
a	- radius of tube
b	- h/R
c_d	- viscous damping coefficient
g	- gravity
$\bar{g}$	- $g/R\Omega^2$
h	- height of annulus above satellite center of mass
k	- $(\sin(\gamma/2))/(\gamma/2)$
m	- mass of fluid
p,q,r	- dimensionless angular velocity components
t	- time
δ	- offset of center of annulus from spin axis
$\bar{\delta}$	- δ/R
ϵ	- $mR^2/A\bar{\gamma}$
γ	- angle of fill of fluid in annulus
$\bar{\gamma}$	- fraction fill, $\bar{\gamma} = \gamma/2\pi$
η	- dimensionless damping coefficient
ν	- angular position of offset in transverse plane
$\bar{\nu}$	- kinematic coefficient of viscosity
Ω	- initial spin rate
$\underset{\sim}{\omega}$	- angular velocity with components ω_u, ω_v, ω_z
ω_t	- transverse angular velocity
τ	dimensionless time, $\tau = \Omega t$

σ_1	- C/A
σ_2	- C/B
σ_{12}	- σ_1/σ_2
θ	- mutation angle
ϕ	- precession angle
ψ	- Euler angle
β	- angular position of slug

1. Introduction

A ring partially filled with a viscous fluid such as mercury was one of the first nutation dampers used on spinning satellites. The first analysis of the partially filled viscous ring damper was performed by Carrier and Miles[1,2]. They assumed that the motion of the damper did not appreciably affect the precession rate of the satellite but acted only as a source of energy dissipation. With this assumption the motion of the fluid in the tube was then treated as a fluid mechanics problem and an approximate solution to the Navier Stokes equations was obtained. Their solution showed that the fluid behaved as a rigid slug for a nutation angle greater than one degree. At these large nutation angles the problem was then treated as boundary layer flow over a flat plate with the width of the plate being equal to the perimeter of the tube. However this analysis did not completely treat the problem as there are two distinctive modes of motion for a nutation angle θ greater than one degree, and in one of these the fluid does not behave like boundary layer flow. The next analysis was performed by Carwright[3,4], et. al., in which they assumed the fluid mass behaved like a particle of equal mass moving in a tube with a viscous damping force. Their analysis revealed that there are two distinctive modes of motion which they called the nutation synchronous mode and the spin synchronous mode. Although there were some minor errors in their equations of motion they correctly analyzed the nutation synchronous mode but failed to analyze the spin synchronous mode.

Interest was revived in this problem when the failure of the

ATS-5 satellite was attributed to the energy dissipation caused by fluid motion in the heat pipes. Consequently it was desirable to be able to predict more accurately the energy dissipation in this type of damper. Also other satellites such as Helios will employ partially filled rings for nutation dampers but during a portion of the flight the satellite will be spinning about an axis of minimum moment of inertia. Since this is an unstable configuration it is very important to be able to predict the rate of energy dissipaton.

As a result Alfriend[5] approached the problem in the same manner as Cartwright[3,4] and obtained equations which approximately describe the motion in both the nutation and spin synchronous modes. The problem with this approach is that it must be accompanied with a method for calculating the damping constant. Leibold[6] suggested assuming steady flow in straight pipe as a means of calculating this damping constant. However there is an error in his equation describing the motion of the satellite.

In this study the fluid is assumed to behave as a rigid slug but but since the fluid may fill up to 50% of the ring it is assumed the fluid is a rigid slug of finite length, not a particle.

In Section 2 a description of the mathematical model is given and for a symmetric satellite approximate solutions are derived for the nutation angle time history and corresponding time constants in both the nutation synchronous and spin synchronous modes. These approximate solutions are then compared to those obtained by numerical integration of the exact equations of motion. In Section 2.2 the effect of a small offset of the center of the ring from the spin axis is investigated. This is necessary since an offset of 1/4" is planned on the

Helios satellite. An analysis of the test data was a part of this investigation so the effect of gravity on the nutational behavior is investigated in Section 2.3. An investigation of the effect of a stop in the tube is investigated in Section 2.4. In Section 2.5 the results of Section 2.1 are extended to the asymmetric satellite.

Several possible methods for determining the damping constant are given in Section 3. An analysis of the test results is presented in Section 4. Finally a summary of the results and conclusions are given in Section 5

2. Statement of the Problem

In the presentation of the analytical results the simplest problem, which is the symmetric satellite with no gravity and no ring offset, is solved first. The effects of gravity and ring offset on the dymmetric satellite problem are then determined. Finally the solution of the asymmetric satellite with no ring offset and no gravity is given. The symmetric problem is considered first rather than solving the asymmetric problem and simplifying the results for the symmetric case because by solving the symmetric problem first one gains more insight into the problem.

The mathematical model is an asymmetric rigid body (satellite) with principal moments of inertia A, B and C and corresponding principal axes represented by the x, y and z axes shown in Figure 1. The z axis is the spin axis. A tube of radius R is attached to the rigid body at the point $(\delta\cos\nu, \delta\sin\nu, h)$. δ is the offset of the center of the ring (tube) from the spin axis. Moving in the tube is a rigid slug of mass m which fills a portion of the tube, the angle of fill being γ. The other assumptions in the development of the equations of motion are 1) the center of mass of the system and the center of mass of the satellite are coincident, 2) the friction force on the fluid slug can be represented by a linear viscous force, and 3) gravity acts only on the fluid slug. The first assumption is made because it simplifies the equations of motion considerably and the effect of the motion of the system center of mass is negligible since it is of $O(\epsilon^2)$ where ϵ is a small parameter which is defined later. Also, in the tests the satellite center of mass is a fixed point. The third assumption is made since gravity has an effect only in the tests and the satellite without the fluid was statically balanced before the tests.

The equations of motion which are derived in Appendix A are

$$\left[\frac{(1+\sigma_{12})}{2}+\frac{(1-\sigma_{12})}{2}\cos 2\beta+I_{uu}\right]p' + \left[-\frac{(1-\sigma_{12})}{2}\sin 2\beta-I_{uv}\right]q'$$

$$-I_{uz}(r'+\beta'') = [-I'_{uu}+(1-\sigma_{12})\sin 2\beta]p\beta' + [I'_{uv}+(1-\sigma_{12})\cos 2\beta]q\beta' \qquad (2.1)$$

$$+ I'_{uz}(r+\beta')\beta' + (r+\beta')\bar{H}_v - q\bar{H}_z + \bar{M}_u$$

$$\left[-\frac{(1-\sigma_{12})}{2}\sin 2\beta-I_{uv}\right]p' + \left[\frac{(1+\sigma_{12})}{2}-\frac{(1-\sigma_{12})}{2}\cos 2\beta+I_{vv}\right]q'-I_{vz}(r'+\beta'')$$

$$= \left[\frac{(1-\sigma_{12})}{2}\cos 2\beta+I'_{uv}\right]p\beta' + [-I'_{vv}-(1-\sigma_{12})\sin 2\beta]q\beta' + I'_{vz}(r+\beta')\beta' \qquad (2.2)$$

$$+ p\bar{H}_z - (r+\beta')\bar{H}_u + \bar{M}_v$$

$$- I_{uz}p' - I_{vz}q' + (\sigma_1+I_{zz})r' + I_{zz}\beta'' = I'_{uz}p\beta' + I'_{vz}q\beta'$$

$$- I_{zz}(r+\beta')\beta' + q\bar{H}_u - p\bar{H}_v + \bar{M}_z \qquad (2.3)$$

$$-bkp' + (1+\bar{\delta}k\cos(\beta-\nu))r' + \beta'' = -\eta\beta' - \bar{g}k\sin\theta\cos(\psi+\beta)$$

$$+ (\bar{I}_{uu}-\bar{I}_{vv}-\bar{I}'_{uv})pq - bk\,q(r+\beta') + \bar{I}'_{zz}(p^2+r^2) \qquad (2.4)$$

where

$$\bar{H}_\alpha = H_\alpha/A\Omega$$

$$\bar{M}_\alpha = M_\alpha/A\Omega^2 \qquad (2.5)$$

$$I'_{\alpha\omega} = \frac{\partial I_{\alpha\omega}}{\partial\beta}$$

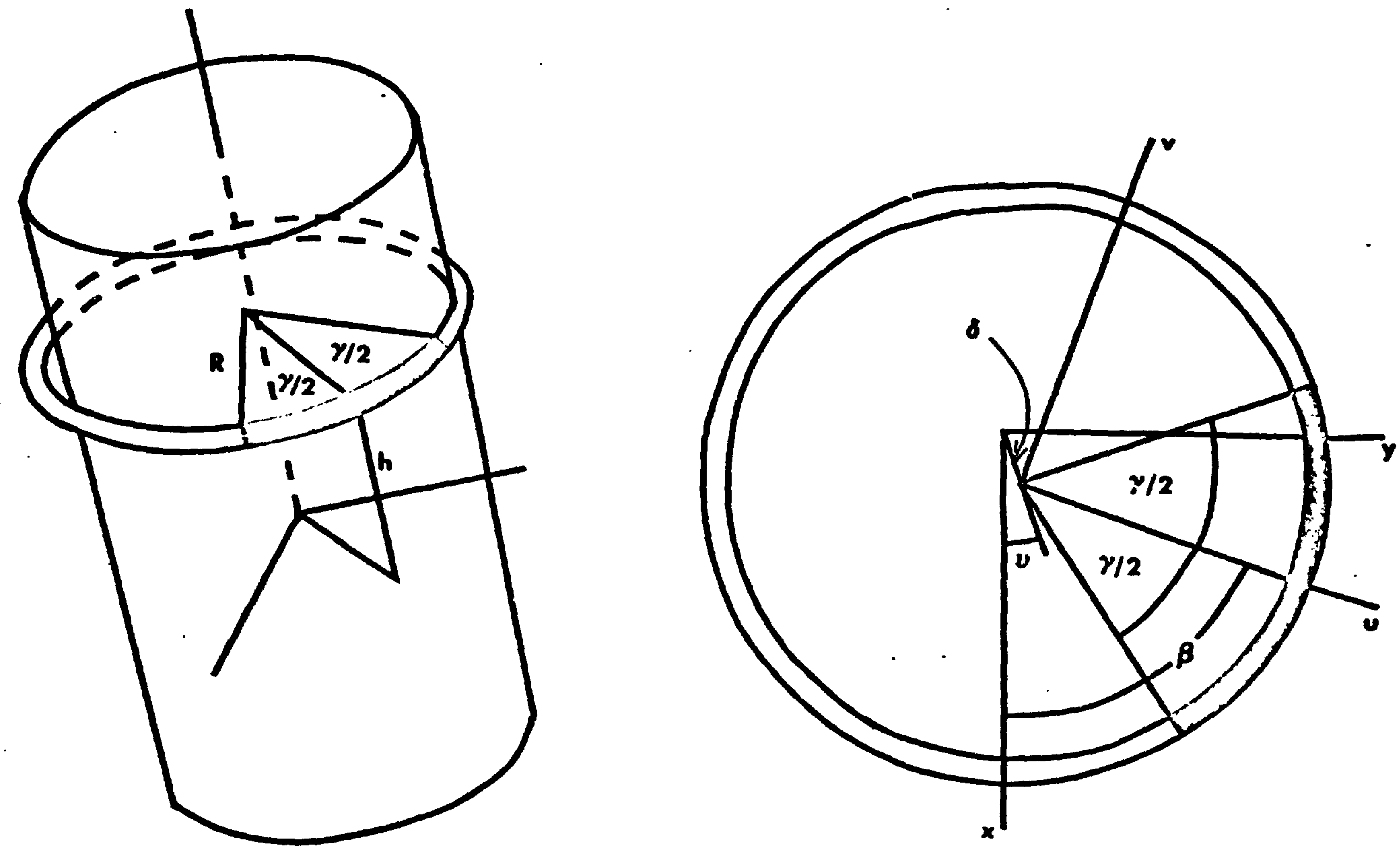

Figure 1. Mathematical Mode Coordinate Systems

The coordinate systems and angles are defined in Figure 1. p, q and r are the components of the dimensionless angular velocity along the u, v and z axes and β defines the position of the slug in the tube. The $I_{\alpha\omega}$ and $J_{\alpha\omega}$ are the moments of inertia of the slug and their derivatives are given in Appendix B. The independent dimensionless parameters of the system are σ_1, σ_2, ϵ, b, η, γ or $\bar{\gamma}$, $\bar{g}$, $\bar{\delta}$ and ν where

$$
\begin{aligned}
\sigma_1 &= C/A \\
\sigma_2 &= C/B \\
\epsilon &= mR^2/A\bar{\gamma} \\
b &= h/R \\
\eta &= c_d/m\Omega \\
\bar{g} &= g/R\Omega^2 \\
\bar{\delta} &= \delta/R
\end{aligned}
\tag{2.6}
$$

Primes denote differentiation with respect to the dimensionless time $\tau = \Omega\tau$ where Ω is the initial spin rate. θ, ψ and ϕ are the Euler angles with θ being the nutation angle and ϕ the precession angle. The Euler angles are determined from

$$\theta' = p\cos(\psi+\beta) - q\sin(\psi+\beta) \tag{2.7}$$

$$\phi' = [p\sin(\psi+\beta) + q\cos(\psi+\beta)]/\sin\theta \tag{2.8}$$

$$\psi' = r - \phi'\cos\theta \tag{2.9}$$

2.1 Symmetric Satellite with Zero Offset and Zero Gravity

Since there are no external forces the angular momentum is constant. Letting the reference direction be $\underset{\sim}{N}_z$ (the vertical when gravity is present) the nutation angle θ can be determined from

$$\tan\theta = \frac{H_t}{H_z} \tag{2.10}$$

instead of using (2.7). H_z is the spin axis component of the angular momentum and H_t is the transverse component, i.e.,

$$H_t^2 = H_u^2 + H_v^2 \quad . \tag{2.11}$$

Substituting for H_u and H_v and expanding in a power series in ϵ gives

$$\tan\theta = \frac{\omega_t}{\sigma} + O(\epsilon) \tag{2.12}$$

where

$$\begin{aligned} \omega_t^2 &= p^2 + q^2 \\ \sigma &= \sigma_1 = \sigma_2 \end{aligned} \tag{2.13}$$

However to use (2.10) to obtain the variation of θ one would have to obtain p, q and r through $O(\epsilon)$, which is no easy task. Rather than using (2.10) or (2.12) one can obtain a good approximation of θ by differentiating (2.10) and then integrating the resulting differential equation. Differentiation of (2.10) gives

$$\theta' = \frac{H_t'}{H_z} = -\frac{H_z'}{H_t} = \frac{pH_v - qH_u}{H_t} \tag{2.14}$$

Substituting for H_u and H_v and expanding in a power series in ϵ yields

$$\theta' = [\frac{\sin}{2} p + (1+\beta')b \sin(\gamma/2)]\frac{\epsilon q}{\pi\omega_t} + O(\epsilon^2) \tag{2.15}$$

The advantage of (2.15) is that to determine θ to $O(\epsilon)$ one only needs the first approximation of p, q and β.

<u>Damper Motion</u>

A symmetric rigid body which is spinning about its axis of symmetry has a constant nutation angle when no damping is present. The transverse angular velocity vector $\underset{\sim}{\omega}_t$ rotates at a rate of $\sigma\Omega\cos\theta$ and the body rotates relative to $\underset{\sim}{\omega}_t$ at a rate of $(1-\sigma)\Omega$. When no damping is present the center of mass of the fluid slug will be flung outward as far as possible which will be along $\underset{\sim}{\omega}_t$ or the plane formed by $\underset{\sim}{H}$ and the z axis, hereafter called the nutation plane. The fluid slug will then be moving at a constant rate of $(1-\sigma)\Omega$ with respect to the body. Introduction of a small amount of damping causes the center of mass of the fluid slug to move off the nutation plane to an equilibrium position where a component of the centrifugal force balances the friction force. This type of motion is called "nutation synchronous" motion[3]. In this mode the fluid slug is moving at a constant rate with respect to the body, hence the energy dissipation rate is a constant. If $\sigma > 1$ the nutation angle decreases which causes a decrease in the centrifugal force and the fluid slug center of mass moves further from the nutation plane. Eventually the centrifugal force is not large enough to balance the damping force and the fluid slug begins to be dragged around with the body while oscillating in the tube. This type of motion is called spin-synchronous motion.

The purpose now is to determine the behavior of the nutation angle in these two modes as a function of the dimensionless parameters $\epsilon, \eta, b, \sigma$ and γ.

Nutation Synchronous Mode

Expanding the equations of motion, Equations (2.1)-(2.4), in a power series in ϵ and dropping all terms of $O(\epsilon)$ gives

$$r = 1 \tag{2.16a}$$

$$p' + (\lambda-\beta')q = 0 \tag{2.16b}$$

$$q' - (\lambda-\beta')p = 0 \tag{2.16c}$$

$$\beta'' + \eta\beta' + \frac{\sin\gamma}{\gamma}pq + b\sigma q(\sin(\gamma/2))/(\gamma/2) = 0 \tag{2.16d}$$

where $\lambda = \sigma - 1$.

Letting

$$\alpha = \beta - \lambda\tau \tag{2.17}$$

the solution to (2.16b) and (2.16c) is

$$p = -\omega_t \cos \alpha$$

$$q = \omega_t \sin\alpha \tag{2.18}$$

where it has been assumed that $q = 0$ and $\beta = 0$ at $\tau = 0$. Thus α measures the position of the center of mass of the fluid slug with respect to the nutation plane. Substituting (2.17) and (2.18) into (2.16d) gives

$$\alpha'' + \eta\alpha' + b\sigma\omega_t \sin\alpha\,(\sin(\gamma/2))/(\gamma/2)[1 - \frac{\omega_t\cos(\gamma/2)\cos\alpha}{b\sigma}] = -\eta\lambda \tag{2.19}$$

A particular solution of this equation is $\alpha = \alpha_e$ where

$$\sin\alpha_e [1 - \frac{\tan\theta\cos(\gamma/2)\cos\alpha_e}{b}] = -\frac{\eta\bar{\gamma}(\sigma-1)\pi}{b\sigma^2\tan\theta\sin(\gamma/2)} \tag{2.20}$$

where $\omega_t = \sigma\tan\theta$ has been used. Thus the fluid slug will remain in the nutation synchronous mode as long as (2.20) is satisfied. Once θ

becomes small enough so that $\alpha_e = \pm \pi/2$ the fluid slug goes into the spin synchronous mode. The transition angle θ_t from one mode to the other is

$$\tan\theta_t = \frac{\eta|\sigma-1|}{b\sigma^2 \frac{\sin(\gamma/2)}{(\gamma/2)}} \qquad (2.21)$$

Substituting for p and q in (2.15) gives

$$\theta' = \left[1 - \frac{\sigma\tan\theta\cos(\gamma/2)\cos\alpha}{b(\sigma+\alpha')}\right]\frac{\epsilon\sigma b}{\pi}\sin\alpha\sin(\gamma/2) + O(\epsilon^2) \qquad (2.22)$$

Substituting $\alpha = \alpha_e$ and dropping terms of $O(\epsilon^2)$ one obtains

$$\tan\theta\ \theta' = -\frac{\epsilon\eta\bar{\gamma}(\sigma-1)}{\sigma} \qquad (2.23)$$

for which the solution is

$$\cos\theta = \cos\theta_o \exp(\tau/\tau_{cn}) \qquad (2.24)$$

where

$$\tau_{cn} = \frac{\sigma}{\epsilon\eta\bar{\gamma}(\sigma-1)} \qquad (2.25)$$

Thus in the nutation synchronous mode the cosine of the nutation angle exhibits exponential behavior. If there are N dampers the time constant is

$$\tau_{cn} = \frac{\sigma}{(\sigma-1)}/(\sum_{i=1}^{N}\epsilon_i\eta_i\bar{\gamma}_i) \qquad (2.26)$$

It has not been assumed that θ is small thus (2.24) is valid for $0 < \theta < \pi/2$. For small θ the nutation angle time history is

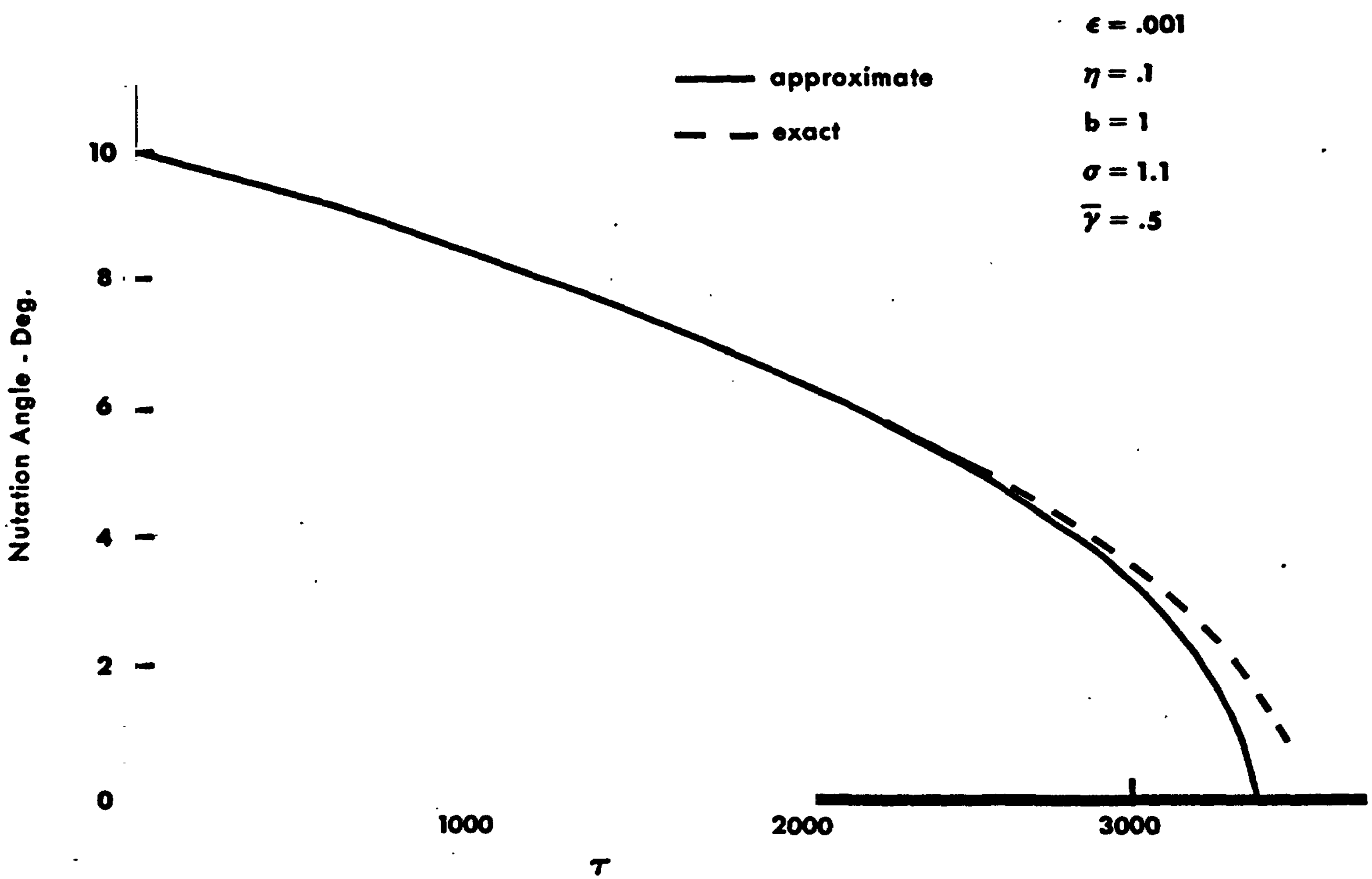

Figure 2. Exact and Approximate Nutation Angle Time Histories for the Nutation Synchronous Mode

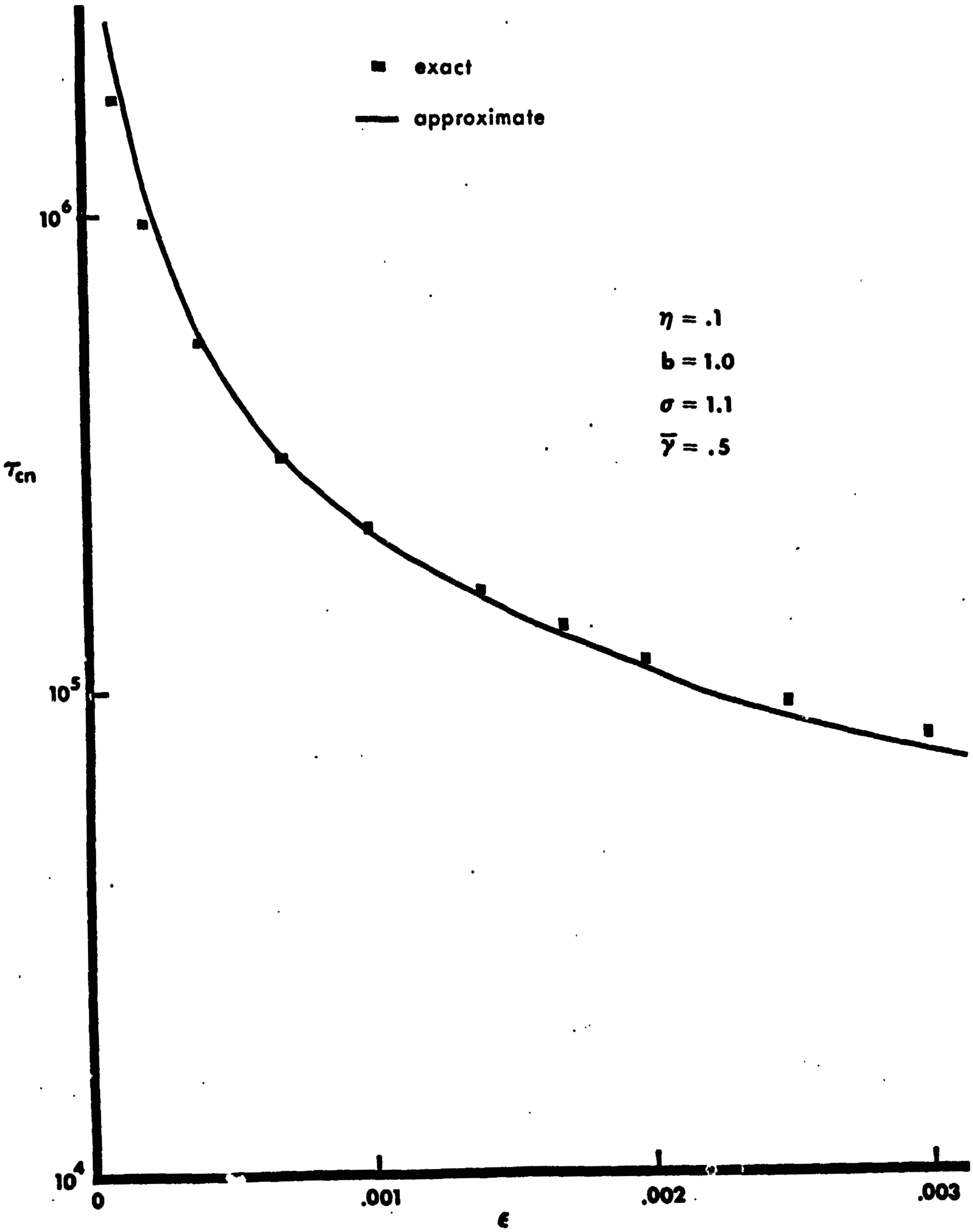

Figure 3. τ_{cn} vs. ϵ

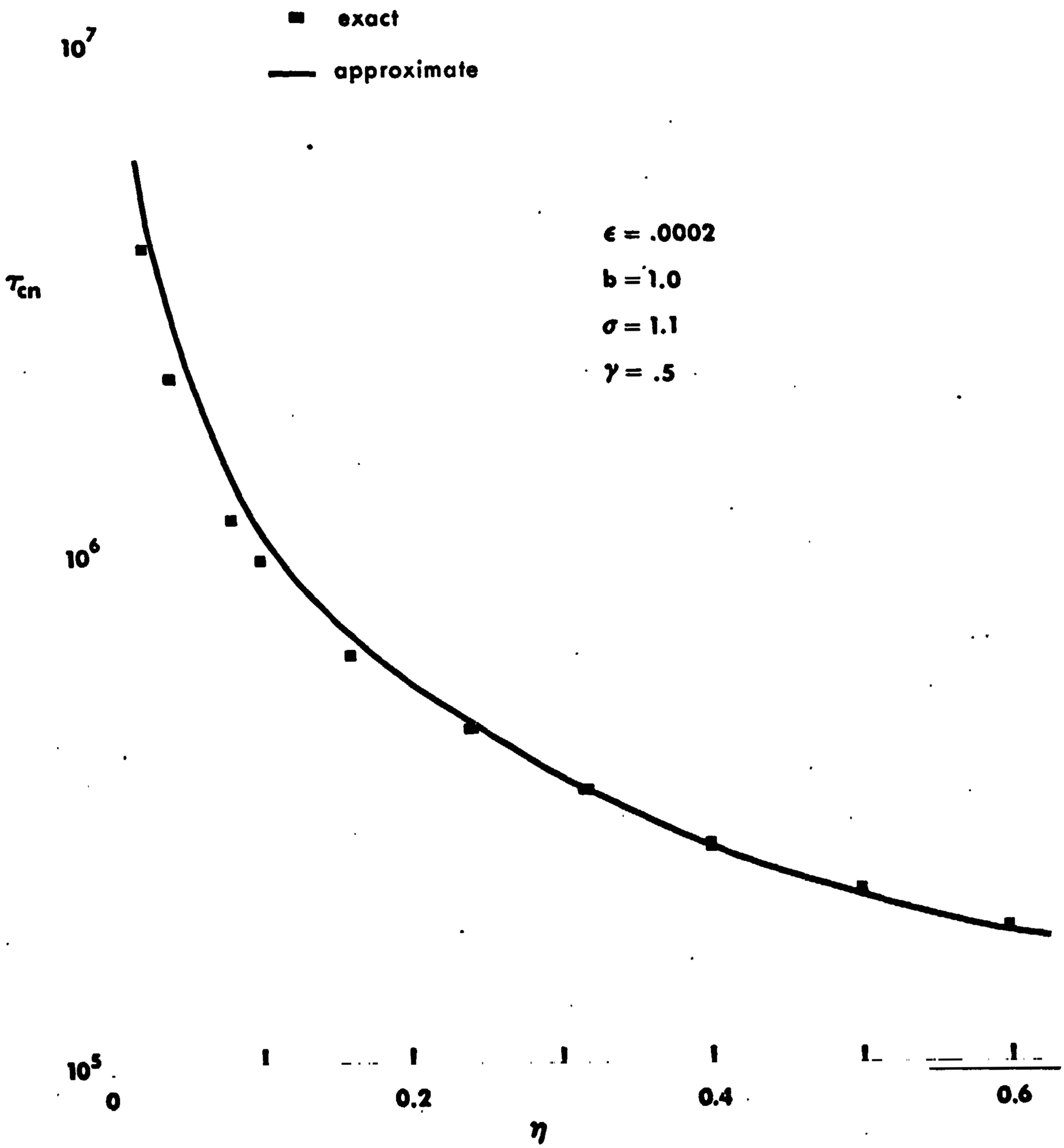

Figure 4. τ_{cn} vs. η

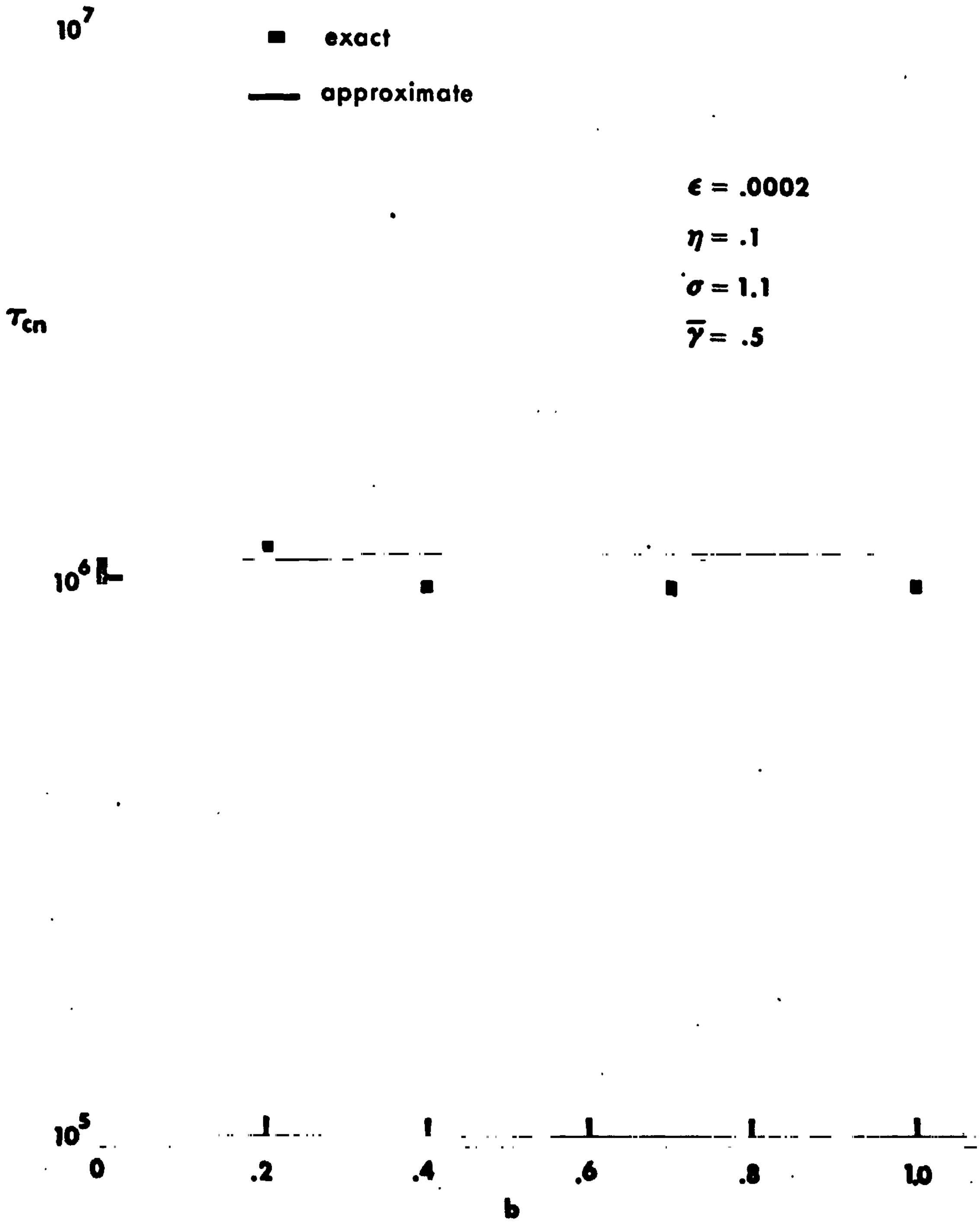

Figure 5. τ_{cn} vs. b

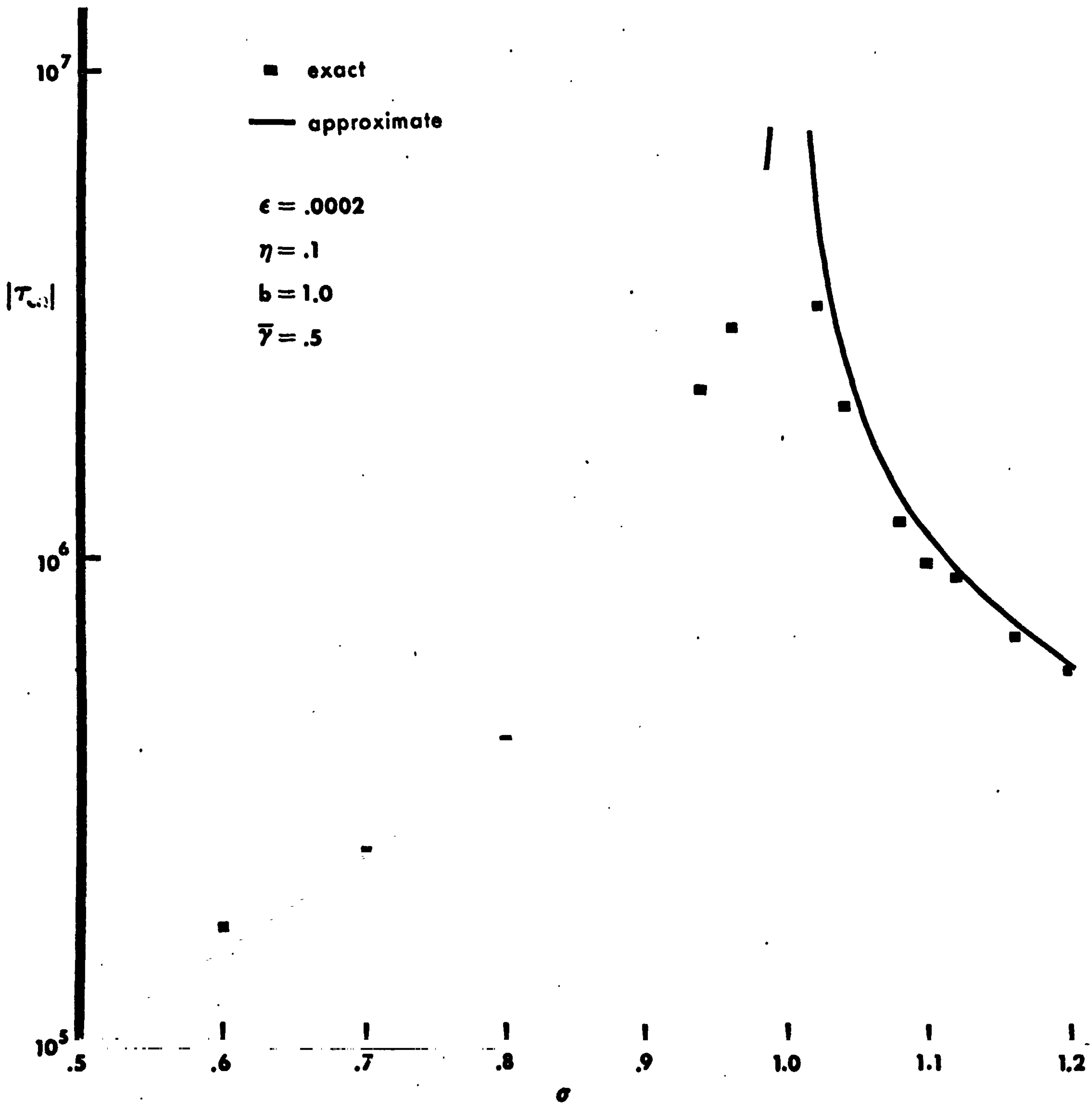

Figure 6. $|\tau_{cn}|$ vs. σ

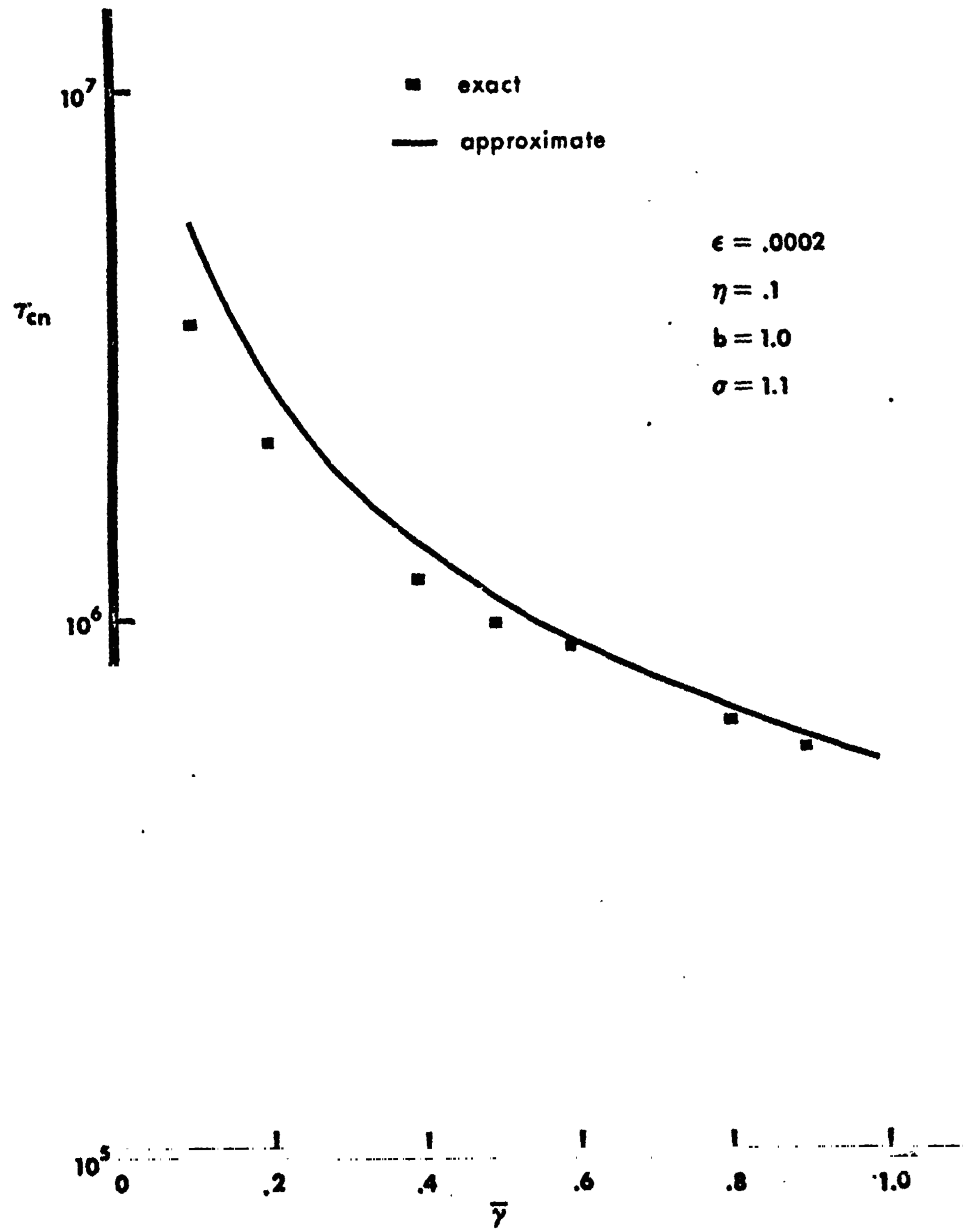

Figure 7. τ_{cn} vs. $\overline{y}$

$$\theta = \theta_o \left(1 - \frac{2\tau}{\tau_{cn}\theta_o^2}\right)^{1/2} \tag{2.27}$$

A comparison of the approximate solution given by (2.24), to the exact solution is shown in Figure 2. A comparison of the time constant given by Equation (2.25) and an exact* time constant obtained by integrating the equations of motion, Equations (2.1)-(2.4), is given in Figures 3-7.

Spin Synchronous Motion

Substituting (2.18) into (2.16d) yields

$$\beta'' + \eta\beta' + \frac{2b\sigma}{\gamma}\omega_t \sin(\gamma/2)\sin(\beta-\lambda\tau)\left[1 - \frac{\omega_t\cos(\gamma/2)\cos(\beta-\lambda\tau)}{\sigma b}\right] = 0 \tag{2.28}$$

Assuming that $\omega_t \ll 1$ and using the first iterate of a Picard iteration scheme a good first approximation of the steady state solution of Equation (2.28) is

$$\epsilon = \frac{b\sigma^2}{\lambda}\tan\theta\sin(\gamma/2)/(r/2)[E\ \sin(\beta_o-\lambda\tau)+F\ \cos(\beta_o-\lambda\tau)] \tag{2.29}$$

where

$$E = \lambda/[\lambda^2+\eta^2]$$

$$F = \eta/[\lambda^2+\eta^2]$$

The nutation angle differential equation is

$$\theta' = \frac{\epsilon}{\pi}\left[-\frac{\sin\gamma}{\gamma}\omega_t\cos(\beta-\lambda\tau)+(1+\beta')b\ \sin(\gamma/2)\right]\sin(\beta-\lambda\tau)\ . \tag{2.30}$$

---

* The exact time constant is obtained by integrating the exact equations over a suitable period of time, assuming exponential behavior for $\cos\theta$ and calculating the time constant.

Assuming that θ is small enough so that terms of $O(\theta^2)$ can be neglected and assuming that the change in β is small so that $\sin\delta\beta = \delta\beta$ and $\cos\delta\beta = 1$ (2.30) reduces to

$$\theta' + \theta\left(\frac{1}{\tau_{cs}} + \kappa_1\cos 2\lambda\tau + \kappa_2\sin 2\lambda\tau\right) = -\frac{\epsilon b}{\pi}\sin(\gamma/2)\sin\lambda\tau \quad (2.31)$$

where

$$\tau_{cs} = \frac{2(\sigma-1)[(\sigma-1)^2+\eta^2]}{\epsilon b^2\sigma^3\eta\bar{\gamma}\left(\frac{\sin(\gamma/2)}{\gamma/2}\right)^2} \quad (2.32)$$

The solution of (2.31) is an infinite series but the κ_1 and κ_2 terms contribute nothing to the exponential decay of the solution. Thus the important part of the solution is

$$\theta = \theta_o e^{-\tau/\tau_{cs}} + \frac{\epsilon b\sin(\gamma/2)}{\pi(\lambda^2\tau_{cs}^2+1)}[-\tau_{cs}\sin\lambda\tau + \lambda\tau_{cs}^2(\cos\lambda\tau - e^{-\tau/\tau_{cs}})] \quad (2.33)$$

Comparison of τ_{cs} given by (2.32) and the time constant obtained from numerical integration of the exact equations of motion is shown in Figs.8-12.

2.2 Damper Offset Effect

The purpose of having the center of the ring offset from the spin axis is to guarantee that the fluid will act as a rigid slug. The analysis of Carrier and Miles[1,2] showed that for very small mutation angles the fluid would spread out along the outer wall of the tube. However, if there is an offset the centrifugal force will be greatest (for very small mutation angles) in the direction of the offset and the fluid will tend to lump there. Consideration of the physical situation is an aid in determining the effect of the offset. Let the offset angle be the angle between the spin axis and the vector from the satellite center of mass to the center of the ring. For small offsets the offset angle is smaller than the

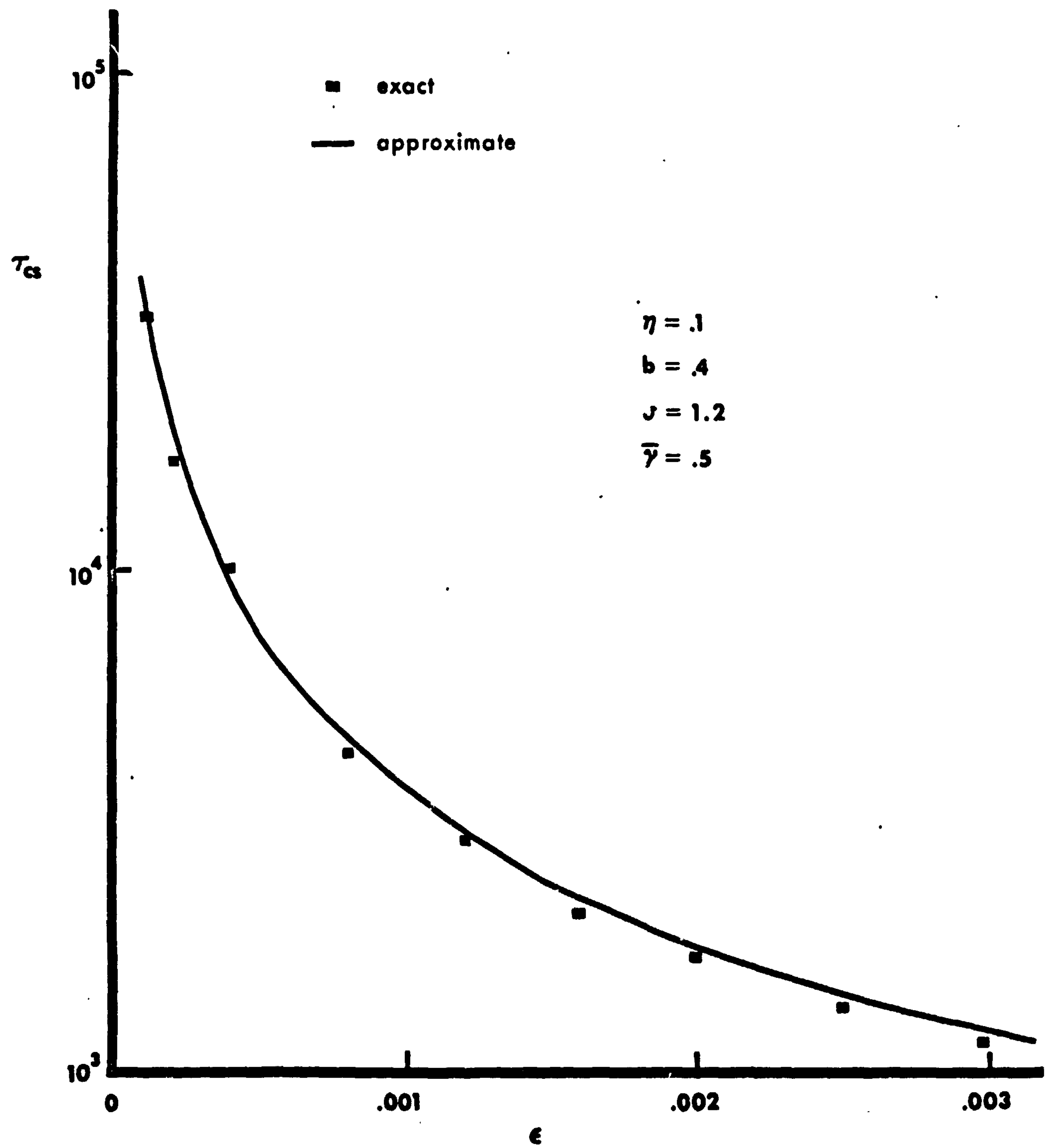

Figure 8. τ_{cs} vs. ϵ

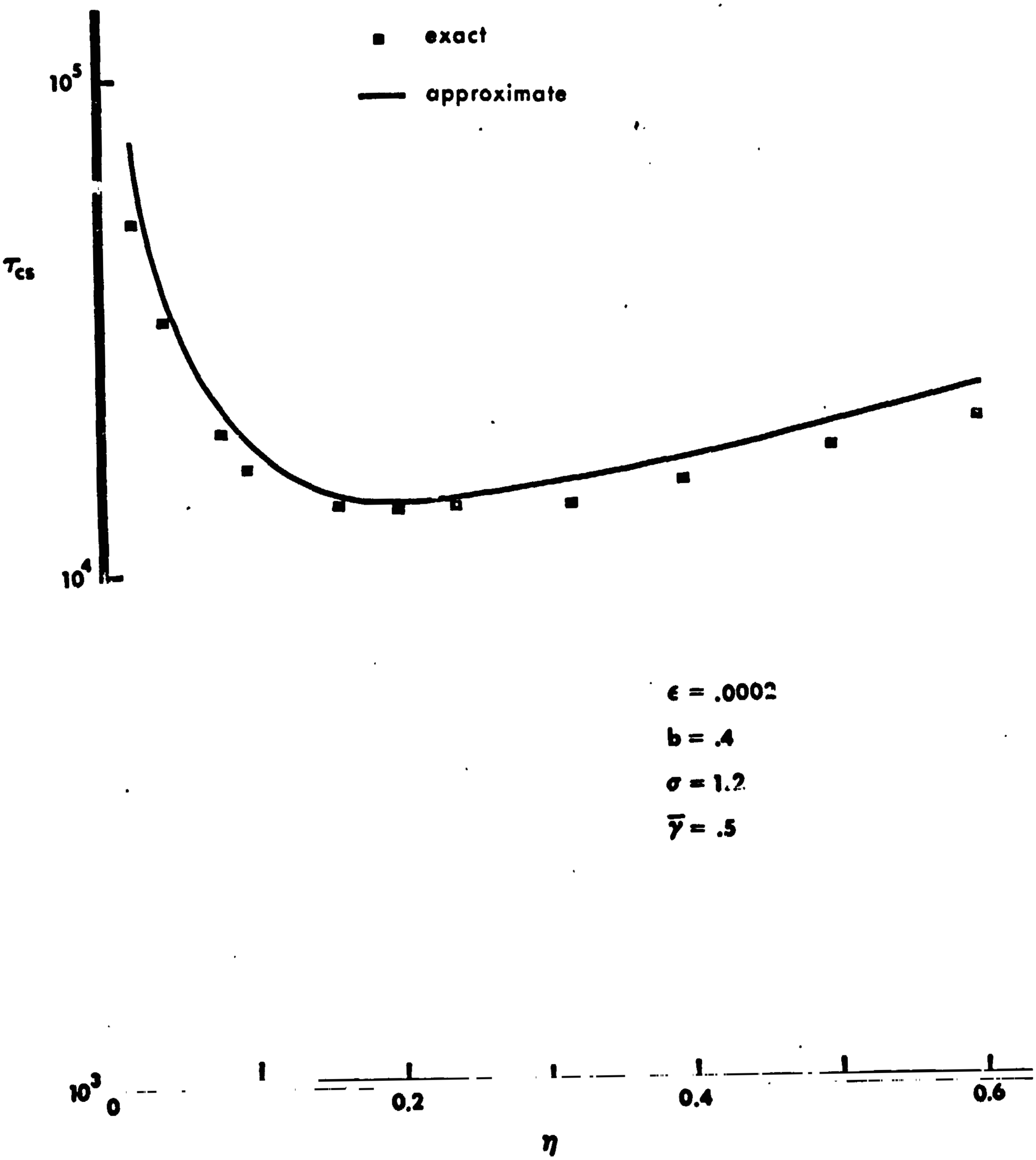

Figure 9. τ_{cs} vs. η

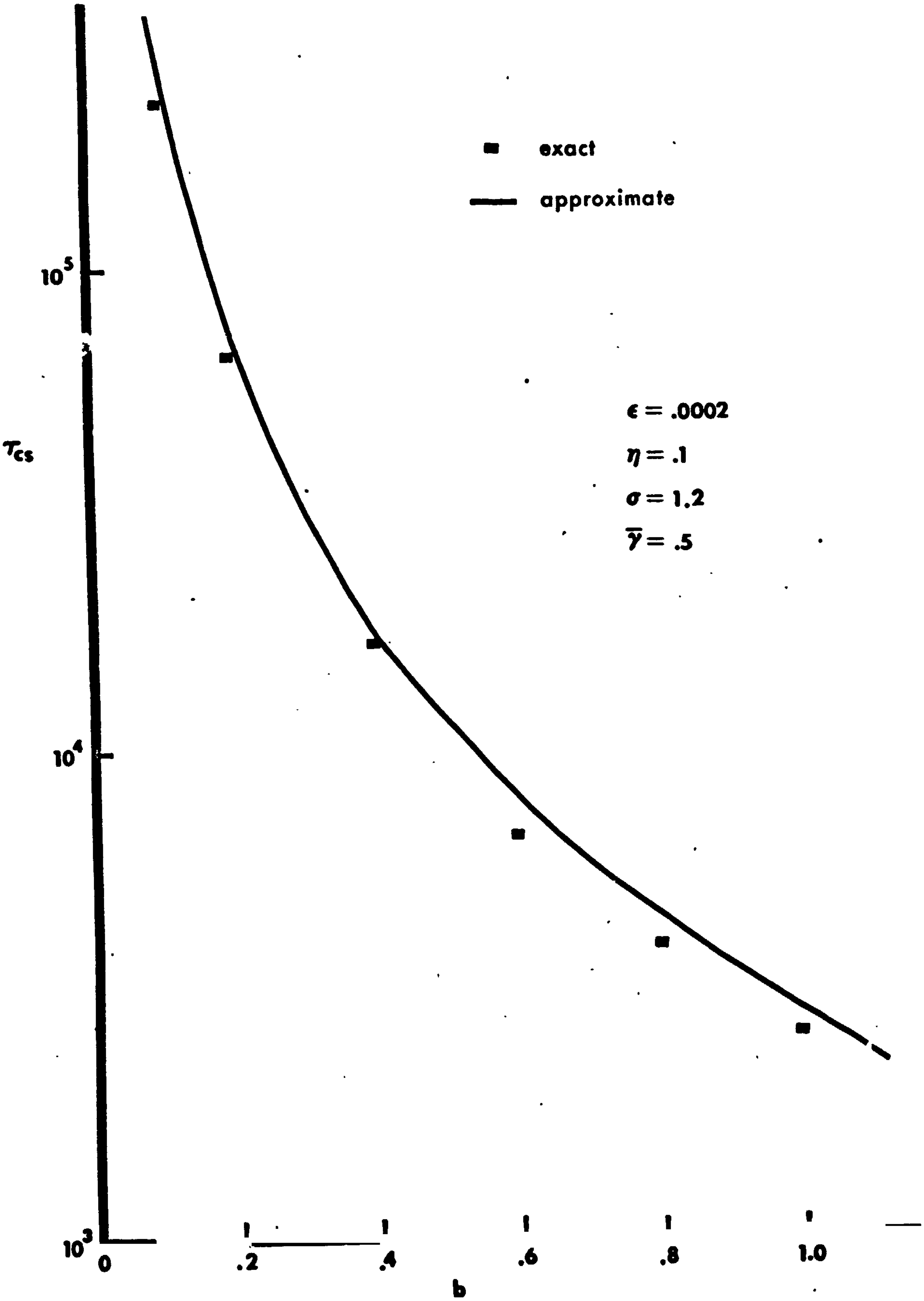

Figure 10. τ_{cs} vs. b

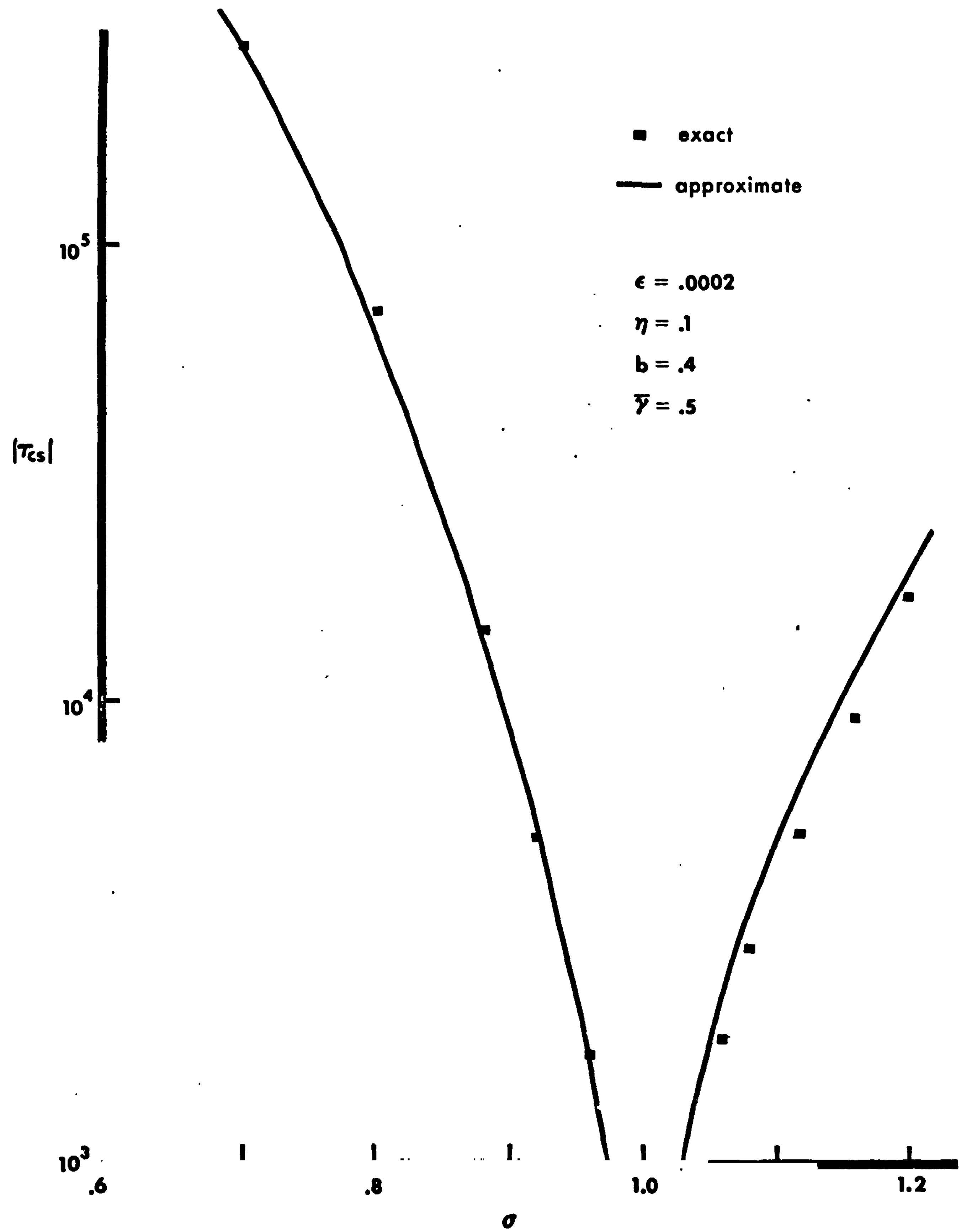

Figure 11. $|\tau_{cs}|$ vs. σ

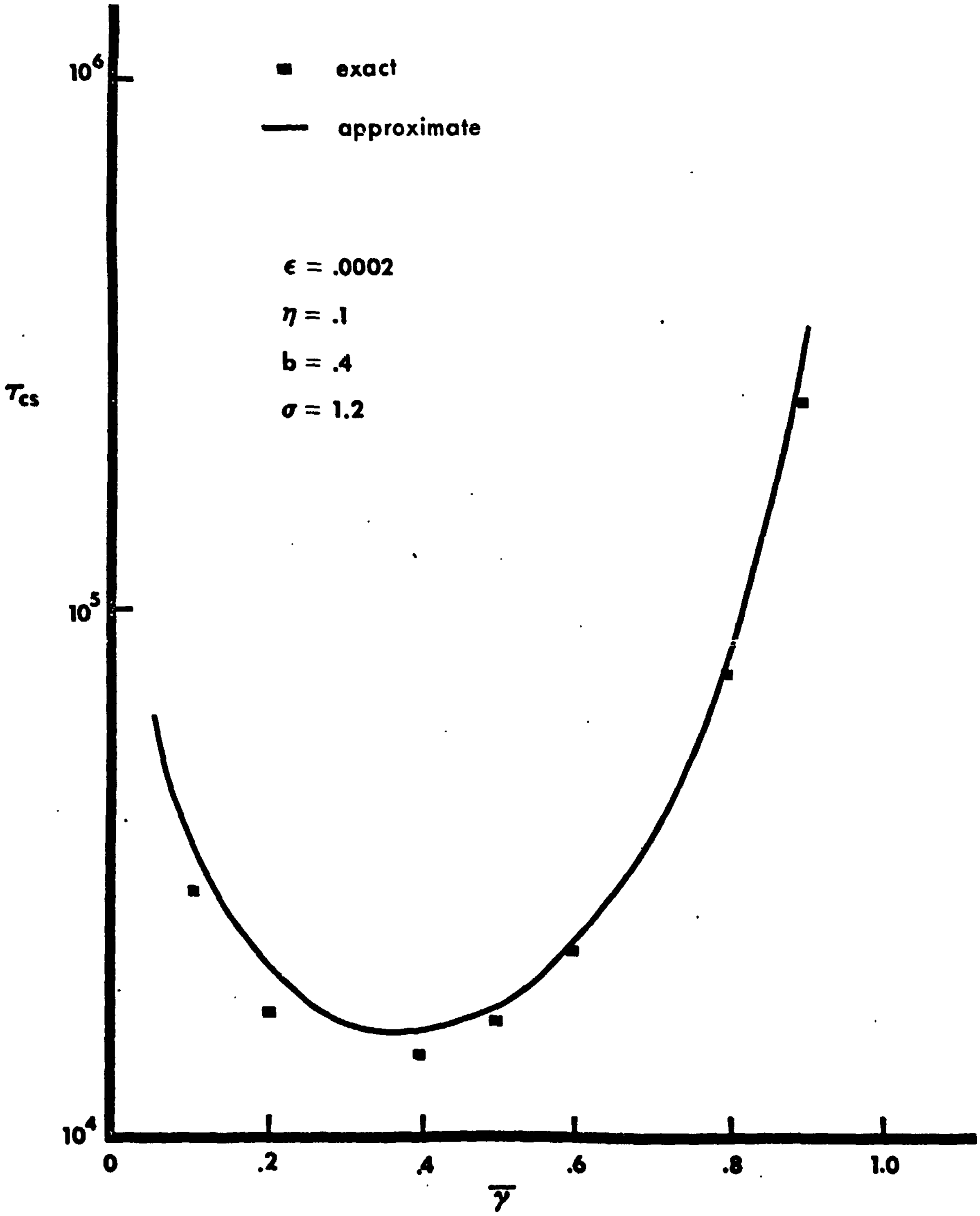

Figure 12. τ_{cs} vs. $\overline{\gamma}$

transition angle. When $\theta > \theta_T$ and no offset the fluid slug maintains a fixed position with respect to the nutation plane since the centrifugal force is constant. The effect of the offset should be to cause small oscillations of the slug about this equilibrium position of the slug. The result would a small change in the rate of energy dissipation which would cause a small change in τ_{cn}. Numerical integration of the equations of motion has verified these conjectures. For the Helios satellite the offset of 1/4" caused less than a 10% change in τ_{cn}. (τ_{cn} decreases since the rate of energy dissepation increases.)

In the spin synchronous mode $(\theta < \theta_T)$ and zero offset the fluid slug moves slowly around the tube while oscillating. Since the offset would create a point in the ring where the centrifugal force is a maximum the fluid slug should oscillate about this point instead of moving slowly around the tube with the result that the change in τ_{cs} should be minimal. Again numerical integration of the equations of motion verified these conjectures. Except for one case the change in τ_{cs} was less than 10% for the Helios satellite with a 1/4" offset. The one exceptional case will be discussed in Section 4.

2.3 Gravity Effect

Since the satellite was balanced without the fluid it is assumed that the gravitational force acts only on the fluid slug. Following the procedure of Section 2.1 the approximate equations of motion are:

$$r = 1 \tag{2.34a}$$

$$p' + (\lambda - \beta')q = 0 \tag{2.34b}$$

$$q' - (\lambda - \beta')p = 0 \tag{2.34c}$$

$$\beta'' + \eta\beta' + \frac{\sin\gamma}{\gamma} p\,q + b\sigma k\,q + k\bar{g}\sin\theta\cos(\beta + \psi) = 0 \tag{2.34d}$$

where θ is the angle between the spin axis and local vertical. Note that the only term involving gravity is the last term of (2.34d). The solution of (2.34b) and (2.34c) is

$$p = -\omega_t \sin(\lambda\tau - \beta)$$
$$q = -\omega_t \cos(\lambda\tau - \beta) \tag{2.35}$$

Since gravity is present the angular momentum is no longer constant, consequently $\underset{\sim}{H}$ does not coincide with the vertical. Let θ_h be the angle between $\underset{\sim}{H}$ and the spin axis. Then

$$\tan\theta_h = \frac{H_t}{H_z} \approx \frac{\omega_t}{\sigma} \tag{2.36}$$

Differentiation yields

$$\theta_h' = \epsilon\bar{\gamma}[\frac{\sin\gamma}{\gamma} p + bk(1+\beta')]\sin(\beta-\lambda\tau) + \epsilon\bar{\gamma}k\bar{g}\sin(\beta-\lambda\tau)\cos\theta_h\cos(\theta-\theta_h) \tag{2.37}$$

where

$$\psi = -\lambda\tau - \pi/2 \tag{2.38}$$

has been used.

The assumption is now made that the change in $(\theta-\theta_h)$ is small compared to the change in θ, and that $\theta = \theta_h$ at $\tau = 0$. This allows one to use $\theta = \theta_h$ in the equations. Numerical integration of the equations of motion shows that this is a reasonable assumption. Equation (2.37) becomes

$$\theta' = \epsilon\bar{\gamma}[\frac{\sin\gamma}{\gamma} p + bk(1+\beta') + k\bar{g}\cos\theta]\sin(\beta-\lambda\tau) \tag{2.39}$$

Nutation Synchronous Mode

As in Section 2.1 define

$$\alpha = \beta - \lambda\tau \tag{2.40}$$

Substitution into (2.34d) gives

$$\alpha'' + \eta\alpha' + [\omega_t b\sigma k + \bar{g}\, k \sin\theta - \frac{\sin\gamma}{\gamma}\omega_t^2 \cos\alpha]\sin\alpha \quad = \quad -\eta\lambda \tag{2.41}$$

There is an equilibrium value $\alpha = \alpha_e$ which is given by

$$[b\sigma^2 k\ \tan\theta(1 + \frac{\bar{g}}{b\sigma^2}\cos\theta) - \sigma^2\tan^2\theta\frac{\sin\gamma}{\gamma}\cos\alpha_e]\sin\alpha_e \quad = \quad -\eta\lambda \tag{2.42}$$

The transition angle between the two modes is obtained by setting $\alpha_e = \pm\ \pi/2$, which gives

$$\tan\theta_T(1 + \frac{\bar{g}}{b\sigma^2}\cos\theta_T) \quad = \quad \frac{\eta(\sigma-1)}{b\sigma^2 k} \tag{2.43}$$

which for small θ becomes

$$\theta_T \quad = \quad \frac{\eta|\sigma-1|}{b\sigma^2 k G} \tag{2.44}$$

where

$$G \quad = \quad 1 + \bar{g}/\sigma^2 b \tag{2.45}$$

Substituting (2.42) into (2.39) yields

$$\tan\theta\ \theta' \quad = \quad \frac{\epsilon\bar{\gamma}\eta(\sigma-1)}{\sigma} \tag{2.46}$$

which is the same equation one obtains without gravity. Thus the only effect gravity has in the nutation synchronous mode is to change the transition angle θ_T. The solution to (2.46) is

$$\cos\theta \quad = \quad \cos\theta_o \exp(\tau/\tau_{cn}) \tag{2.47}$$

where

$$\tau_{cn} \quad = \quad \frac{\sigma}{\epsilon\bar{\gamma}\eta(\sigma-1)} \tag{2.48}$$

Spin Synchronous Mode

Using the procedure of Section 2.1 an approximate solution of (2.34d) for small θ is

$$\delta\beta \quad = \quad K(\lambda\sin(\beta_o - \lambda\tau) - \eta\cos(\beta_o - \lambda\tau)) \tag{2.49}$$

where

$$K = \frac{kb\sigma^2 G\theta}{\lambda(\lambda^2+\eta^2)} \tag{2.50}$$

Substituting into (2.39) and using $\sin\delta\beta = \delta\beta$ and $\cos\delta\beta = 1$ gives

$$\theta' + \frac{1}{\tau_{cs}}\theta = -\epsilon\,\bar{\gamma}bk\ G\ \sin\lambda\tau \tag{2.51}$$

where

$$\tau_{cs} = \frac{2(\sigma-1)[(\sigma-1)^2+\eta^2]}{\epsilon\bar{\gamma}b^2\sigma^3\eta k^2G^2} \tag{2.52}$$

Thus gravity can have a substantial effect on the nutation angle in the spin synchronous mode as the time constant is reduced by a factor $1/G^2$.

The approximate time constants given by (2.48) and (2.52) are compared with those obtained by numerical integration in Figure 13. It is seen that the agreement is very good.

2.4 Effect of Closed Ends in Tubes

The manufacture of heat pipes is simpler if there is a stop (closed end) in the pipe. This analysis has been undertaken to determine if it is advantageous from the standpoint of nutation damping to have a stop in the tube. The physical situation is so complex that it defies an accurate analysis. What happens to the fluid when it impacts the stop is not known, thus a very simplified analysis has been performed to try and determine if the stop increases or decreases energy dissipation.

It is assumed that the fluid slug is a point mass and that its motion is governed by (2.16d). Since the nutation angle is essentially constant over one cycle it is also assumed that the nutation angle is constant. Equation (2.16d) is then integrated over a number of cycles taking into account collisions and the average amount of energy dissipation is then determined. This is then compared to the change in kinetic energy for no stops which can be computed analytically.

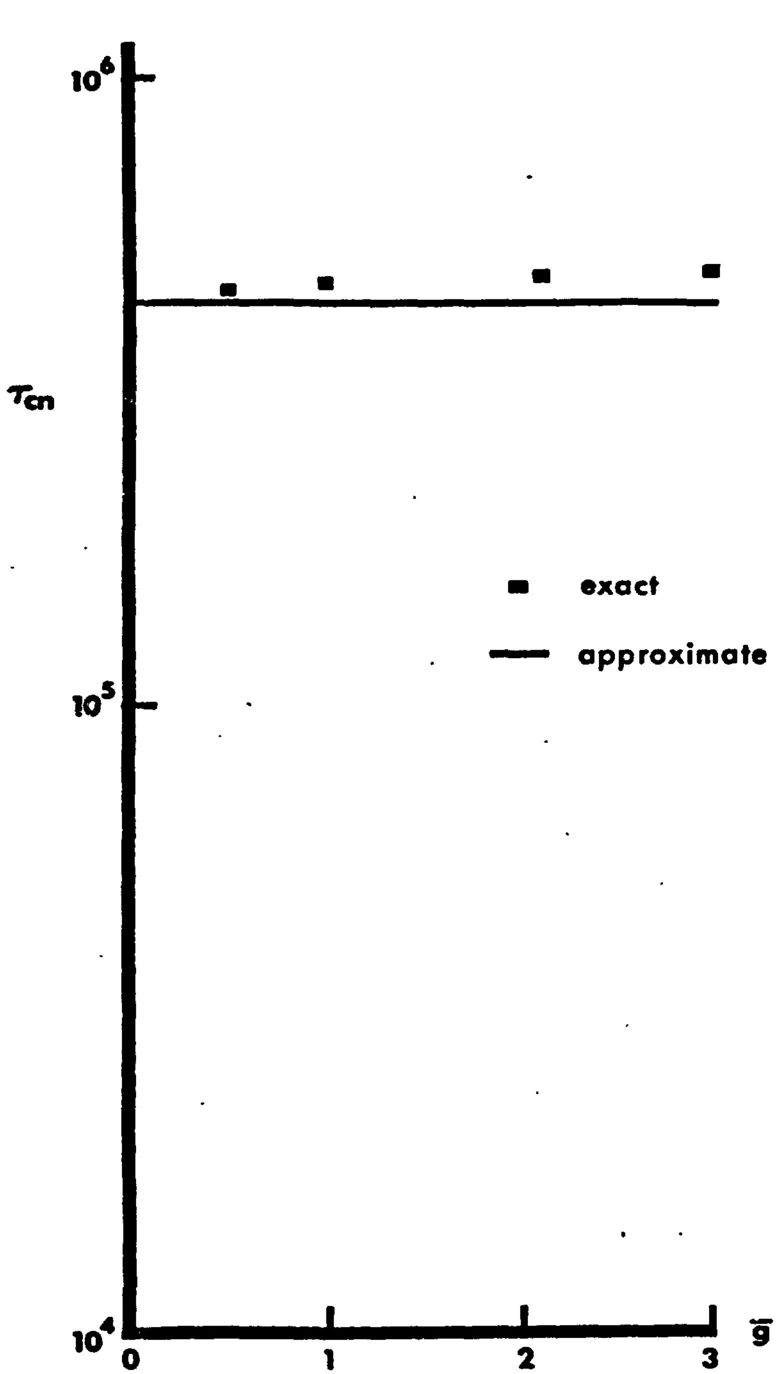

Figure 13a τ_{cn} vs. $\bar{g}$

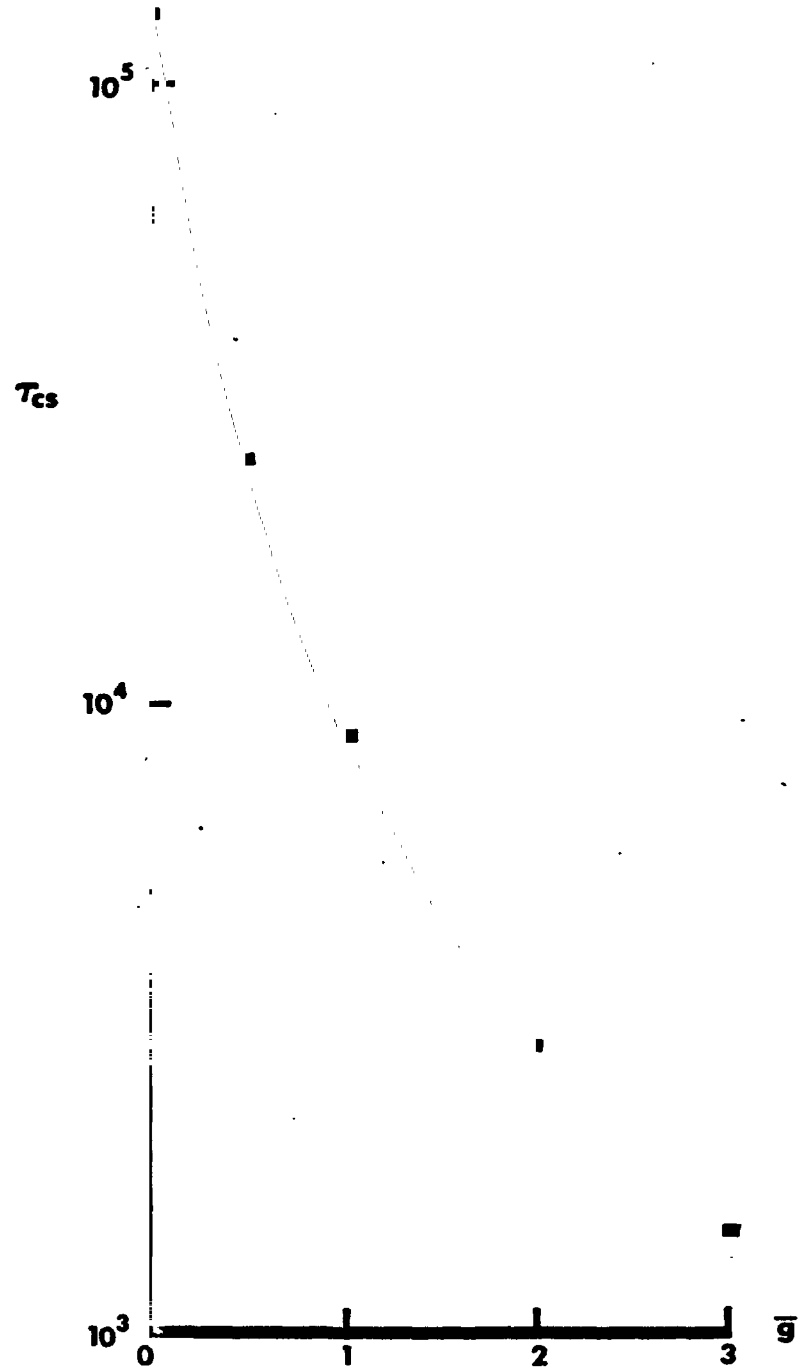

Figure 13b τ_{cs} vs $\bar{g}$

For a continous tube the rate of energy dissipation is

$$\dot{T} = -c_d R^2 \dot{\beta}^2 = -A\epsilon\bar{\gamma}\eta\Omega^3 \beta'^2 \tag{2.53}$$

The change in kinetic energy over one cycle is

$$\Delta T = \int_0^{T_p} \dot{T}\, dt \tag{2.54}$$

where T_p is the period and

$$T_p = \frac{2\pi}{|\sigma-1|\Omega} \tag{2.55}$$

This gives

$$\Delta T = 2\pi \frac{A\epsilon\bar{\gamma}\eta\Omega^2}{|\sigma-1|} \overline{\beta'^2} \tag{2.56}$$

where $\overline{\beta'^2}$ is the average value of β'^2. Let

$$\overline{\Delta T} = \frac{\Delta T}{A\epsilon\bar{\gamma}\Omega^2} \tag{2.57}$$

then

$$\overline{\Delta T} = \frac{2\pi\eta}{|\sigma-1|} \overline{\beta'^2} \tag{2.58}$$

In the nutation synchronous mode

$$\beta' = (1-\sigma)$$

hence

$$\overline{\Delta T} = 2\pi\eta|\sigma-1| \tag{2.59}$$

In the spin synchronous mode.

$$\beta' = \frac{b\sigma^2 k\theta}{(\lambda^2+\eta^2)}[\lambda\cos(\beta_o-\lambda\tau)+\eta\sin(\beta_o-\lambda\tau)]$$

hence

$$\overline{\Delta T} = \frac{\pi b^2\sigma^4 k^2\theta^2\eta}{|\sigma-1|(\lambda^2+\eta^2)} \tag{2.60}$$

The change in kinetic energy when there is a stop in the pipe is obtained by numerical integration of (2.16d) and

$$\dot{\overline{\Delta T}} = \eta\beta'^2 \tag{2.61}$$

To this we have to add the loss in kinetic energy from the collisions which is determined by assuming the slug collides with an object of infinite mass. The loss in kinetic energy ΔT_c from a collision is

$$\overline{\Delta T_c} = \frac{(1-e^2)}{2}\beta_i'^2$$

where e is the coefficient of restitution and β_i' is the angular rate just prior to collision.

Runs were made for both a stable and unstable configuration in the nutation synchronous mode and spin synchronous mode. Table 2.1 gives the results for several values of the coefficient of restitution e. As one can see the change in kinetic energy is relatively independent of e. The increase in energy dissipation is significant in the nutation synchronous mode but small in the spin synchronous mode. This is reasonable since in the nutation synchronous mode the angular rate of the slug with respect to the tube is $|\sigma-1|$ whereas in the spin synchronous mode it is small. In tests run by Hughes Aircraft[10] on the ATS-V heat pipes there was a 40% increase in the change in kinetic energy in the heat pipes with stops. No comparison can be made with the Hughes results because the damping constant η is not known. However one can conclude that putting stops in the rings can cause a substantial increase in the energy dissipation which will result in a decrease in the time constant.

Table 2.1

In all runs $\eta = 0.1$			
Nutation Synchronous $\sigma = 1.2$, $\theta = 6°$, $b = 3$			
e	$\overline{\Delta T}$(no stop)	$\overline{\Delta T}$(1 stop)	% increase in K.E.
0.2	0.126	0.969	670
0.9	0.126	1.002	700
0.6	0.126	1.045	730
0.8	0.126	1.060	740
1.0	0.126	0.839	565
Nutation Synchronous $\sigma = 0.8$, $\theta = 6°$, $b = 3$			
e	$\overline{\Delta T}$(no stop)	$\overline{\Delta T}$(1 stop)	% increase in K.E.
0.2	0.126	0.377	200
0.4	0.126	0.391	210
0.6	0.126	0.403	220
0.8	0.126	0.431	240
1.0	0.126	0.520	313
Spin Synchronous $\sigma = 1.2$, $\theta = 1°$, $b = 0.8$			
e	$\overline{\Delta T}$(no stop)	$\overline{\Delta T}$(1 stop)	% increase in K.E.
0.2	0.0127	0.0162	27
0.4	0.0127	0.0163	28
0.6	0.0127	0.0166	31
0.8	0.0127	0.0163	28
1.0	0.0127	0.0178	40
Spin Synchronous $\sigma = 0.8$, $\theta = 1°$, $b = 0.8$			
e	$\overline{\Delta T}$(no stop)	$\overline{\Delta T}$(1 stop)	% increase in K.E.
0.2	0.0039	0.0048	23
0.4	0.0039	0.0045	15
0.6	0.0039	0.0045	15
0.8	0.0039	0.0048	23
1.0	0.0039	0.0040	3

2.5 Asymmetric Satellite with Zero Offset and Zero Gravity

In developing the approximate solution for the asymmetric satellite it is advantageous to use the components of the angular velocity along the x and y axes rather than the u and v axes. Let p_x and q_y be the dimensionless components of the angular velocity along the x and y axes, then

$$
\begin{aligned}
p_x &= p\cos\beta - q\sin\beta \\
q_y &= p\sin\beta + q\cos\beta
\end{aligned}
\tag{2.62}
$$

Using the same procedure as in Appendix A the equations of motion become

$$
\begin{aligned}
p_x' + (\sigma_1 - \sigma_{12})q_y r = \epsilon\bar{\gamma}\Bigg\{ & \frac{(\bar{I}_{uu}+\bar{I}_{vv})}{2}(-p_x'+q_y r) \\
& + \frac{(\bar{I}_{uu}-\bar{I}_{vv})}{2}[(-p_x'-q_y r-2q_y\beta')\cos 2\beta \\
& \qquad +(-q_y'+p_x r+2p_x\beta')\sin 2\beta] - \bar{I}_{zz}q_y(r+\beta') \\
& + \bar{I}_{uz}[(r'+\beta'')\cos\beta-(r+\beta')^2\sin\beta+q_y(p_x\cos\beta+q_y\sin\beta]\Bigg\}
\end{aligned}
\tag{2.63a}
$$

$$
\begin{aligned}
\sigma_{12}q_y' + (1-\sigma_1)p_x r = \epsilon\bar{\gamma}\ & \frac{(\bar{I}_{uu}+\bar{I}_{vv})}{2}(-q_y'-p_x r) \\
& + \frac{(\bar{I}_{uu}-\bar{I}_{vv})}{2}[(+q_y'-p_x r-2\beta' p_x)\cos 2\beta \\
& \qquad +(-p_x'-q_y r-2\beta' q_y)\sin 2\beta] \\
& + \bar{I}_{zz}p_x(r+\beta') + \bar{I}_{uz}[(r'+\beta'')\sin\beta+(r+\beta')^2\cos\beta \\
& \qquad -p_x(p_x\cos\beta+q_y\sin\beta)]
\end{aligned}
\tag{2.63b}
$$

$$\sigma_1 r' + (\sigma_{12}-1)q_y p_x = \epsilon\bar{\gamma}\eta\beta' \tag{2.63c}$$

$$\beta'' + \eta\beta' + \frac{(1-\sigma_{12})}{\sigma_1}q_y p_x + \bar{I}_{uz}r[(1+\sigma_1-\sigma_{12})q_y\cos\beta-(1+\sigma_2-\sigma_{21})p_x\sin\beta]$$
$$+\frac{(\bar{I}_{uu}-\bar{I}_{vv})}{2}[(p_x^2-q_y^2)\sin 2\beta-2p_x q_x\cos 2\beta] = 0 \tag{2.63d}$$

The method used to obtain the behavior of the nutation angle in the symmetric case can still be applied in the asymmetric case but the resulting expression for θ', Equation (2.14), does not simplify to $\theta' = O(\epsilon)$ because in the asymmetric case θ is not constant when there is no damper. The result is that to use (2.14) higher order approximations of p_x and q_y would have to be developed. To get around this difficulty a variation of parameters approach will be used. When there is no damper the nutation angle θ oscillates, thus the time constant or damping constant obtained will measure the increase or decrease of the maximum value of θ at the end of each oscillation.

For $\epsilon = 0$ the equations of motion for the satellite are

$$p_x' + (\sigma_1-\sigma_{12})q_y r = 0$$

$$q_y' + (\sigma_{21}-\sigma_2)p_x r = 0 \tag{2.64}$$

$$r' + \frac{(\sigma_1-\sigma_2)}{\sigma_1\sigma_2}q_y p_x = 0$$

The solutions for p_x, q_y and r an elliptic functions. It will now be assumed that the nutation angle is small enough or the asymmetry is small enough so that the elliptic functions can be replaced by the first term in their trigonometric expansions. This will limit the approximate solutions to small angles. The approximate solutions when (σ_1-1) and (σ_2-1) have the same sign are

$$\begin{aligned} p_x &= -\omega_t \cos(\lambda\tau+\chi) \\ q_y &= -\omega_t M \sin(\lambda\tau+\chi) \qquad (2.65) \\ r &= 1 \end{aligned}$$

where χ is a phase angle and

$$\begin{aligned} M &= \frac{\sigma_2}{\sigma_1}\left(\frac{\sigma_1-1}{\sigma_2-1}\right)^{1/2} \\ & \qquad\qquad\qquad (2.66) \\ \lambda^2 &= (\sigma_1-1)(\sigma_2-1) \end{aligned}$$

The nutation angle for small angles is given by

$$\theta = \frac{H_T}{H_z} = \frac{(A^2\omega_x^2+B^2\omega_y^2)^{1/2}}{C\omega_z} + O(\epsilon)$$

In terms of the dimensionless variables this becomes

$$\theta = \frac{(p_x^2+\sigma_{12}^2 q_y^2)^{1/2}}{\sigma_1 r}$$

Substituting (2.65) for p_x, q_y, and r gives

$$\theta = [\frac{|\sigma_1+\sigma_2-2|}{2} + \frac{|\sigma_2-\sigma_1|}{2}\cos 2(\lambda\tau+\chi)]^{1/2} \frac{\omega_t}{\sigma_1(\sigma_2-1)^{1/2}} \qquad (2.67)$$

A variation of parameters approach will now be used to obtain ω_t which will then give the approximate nutation angle time history.

Assuming ω_t and χ to be functions of time, substituting for p_x, q_y, r, p_x', q_y' and r' into (2.63a,b) neglecting terms of $O(\epsilon^2)$, linearizing with respect to ω_t, and solving for ω_t' gives the following differential equation for ω_t. [We do not need to solve for χ']

$$\omega_t' = -\epsilon\bar{\gamma}\omega_t \left\{ \frac{(\bar{I}_{uu}+\bar{I}_{vv})}{4\sigma_1\lambda}(\sigma_2-\sigma_1)(\sigma_1\sigma_2+2-\sigma_1-\sigma_2)\sin 2(\lambda\tau+\chi) \right.$$

$$+\frac{(\bar{I}_{uu}-\bar{I}_{vv})}{4\sigma_1\lambda}[(\sigma_1+\sigma_2-\sigma_1\sigma_2)(\sigma_1+\sigma_2-2)+2\beta'(2\sigma_1\sigma_2-\sigma_1-\sigma_2)]\cos 2\beta\sin 2(\lambda\tau+\chi)$$

$$+\frac{(\bar{I}_{uu}-\bar{I}_{vv})}{2\sigma_1}[(\sigma_1\sigma_2-\sigma_1-\sigma_2)-\beta'(\sigma_2+\sigma_1)]\sin 2\beta\cos 2(\lambda\tau+\chi) \tag{2.68}$$

$$+\frac{(\bar{I}_{uu}-\bar{I}_{vv})}{2\sigma_1}(\sigma_2-\sigma_1)\beta'\cos 2(\lambda\tau+\chi)$$

$$+\frac{\bar{I}_{uz}}{\omega_t}[(\beta''\cos\beta-(1+\beta')^2\sin\beta)\cos(\lambda\tau+\chi)+(\beta''\sin\beta+(1+\beta')^2\cos\beta)\frac{\sin(\lambda\tau+\chi)}{\sigma_{12}M}]$$

$$\left. +(1+\beta')\frac{(M-1)}{2}\sin 2(\lambda\tau+\chi)\right\}$$

Spin Synchronous Mode

Substituting (2.65) for p_x and q_y into (2.63d) and neglecting terms of $O(\omega_t^2)$ gives

$$\beta'' + \eta\beta' = \frac{I_{uz}}{\sigma_1}\left[(\sigma_1\sigma_2+\sigma_2-\sigma_1)\left(\frac{\sigma_1-1}{\sigma_2-1}\right)^{1/2}\cos\beta\sin(\lambda\tau+\chi)\right.$$
$$\left.-(\sigma_1\sigma_2+\sigma_1-\sigma_2)\sin\beta\cos(\lambda\tau+\chi)\right]\omega_t \tag{2.69}$$

As in Section (2.1) an approximate steady state solution is developed by using the first iterate of the Picard iteration which is just the solution of (2.69) with $\beta = \beta_o$ on the right-hand side of (2.69).

$$\delta\beta = \beta - \beta_o = K_1\omega_t\cos\beta_o(\eta\cos\lambda\tau+\lambda\sin\lambda\tau) + K_2\omega_t\sin\beta_o(+\eta\sin\lambda\tau-\lambda\cos\lambda\tau) \tag{2.70}$$

$$K_1 = -\frac{I_{uz}(\sigma_1\sigma_2+\sigma_2-\sigma_1)(\sigma_1-1)^{1/2}}{\sigma_1\lambda(\lambda^2+\eta^2)(\sigma_2-1)^{1/2}}$$
$$K_2 = -\frac{I_{uz}(\sigma_1\sigma_2+\sigma_1-\sigma_2)}{\sigma_1\lambda(\lambda^2+\eta^2)} \tag{2.71}$$

Thus the first approximation of β gives an oscillation about β_o with the magnitude of the oscillation proportional to ω_t.

It has been assumed that ω_t is small, hence we can use

$$\sin\beta = \sin\beta_o + \delta\beta\cos\beta_o$$

$$\cos\beta = \cos\beta_o - \delta\beta\sin\beta_o$$

Using these approximations and neglecting terms of $O(\omega_t^2)$ after substituting for β and β' in (2.68) gives

$$\omega_t' + \left[\frac{1}{\tau_{cs}} + \kappa_1 \sin 2(\lambda\tau+\chi) + \kappa_2 \cos 2(\lambda\tau+\chi)\right] \omega_t = \epsilon\bar{\gamma}[\kappa_3 \sin(\lambda\tau+\chi) + \kappa_4 \sin 2(\lambda\tau+\chi)] \tag{2.72}$$

where the κ_i are constants and

$$\frac{1}{\tau_{cs}} = \frac{\epsilon\bar{\gamma}b^2k^2\eta}{2\sigma_1(\lambda^2+\eta^2)} \left[\frac{(\sigma_1\sigma_2+\sigma_2-\sigma_1)^2}{(\sigma_2-1)}\cos^2\beta_o + \frac{(\sigma_1\sigma_2+\sigma_1-\sigma_2)^2}{(\sigma_1-1)}\sin^2\beta_o\right] \tag{2.73}$$

As in Section (2.1) the solution of ω_t is an infinite series but the important part of the solution is the exponential decay given by

$$\omega_t = \bar{\omega}_t e^{-\tau/\tau_{cs}} \tag{2.74}$$

The solution for the nutation angel θ becomes

$$\theta = \left[\frac{|\sigma_1+\sigma_2-2|}{2} + \frac{|\sigma_2-\sigma_1|}{2}\cos 2(\lambda\tau+\chi)\right]^{1/2} \frac{\bar{\omega}_t}{\sigma_1} e^{-\tau/\tau_{cs}} \tag{2.75}$$

Thus the maximum value of θ in each oscillation decays with a time constant of τ_{cs} given by (2.73). Note that τ_{cs} is a function of the position of the slug in the tube as shown by the prescence of β_o in (2.73). Numerical integration and the second iterate in the Picard iteration solution of (2.69) reveal that the slug moves slowly in the tube in addition to its oscillation. The result is that τ_{cs} is a slowly varying function of time. For a design criteria one should use the value of β_o which gives the maximum time constant.

Comparison of (2.73) with an "exact" time constant obtained from the exact equations of motion is given in Figure 14. The comparison is made for $\beta_o = 0$. In the numerical integration a very small offset

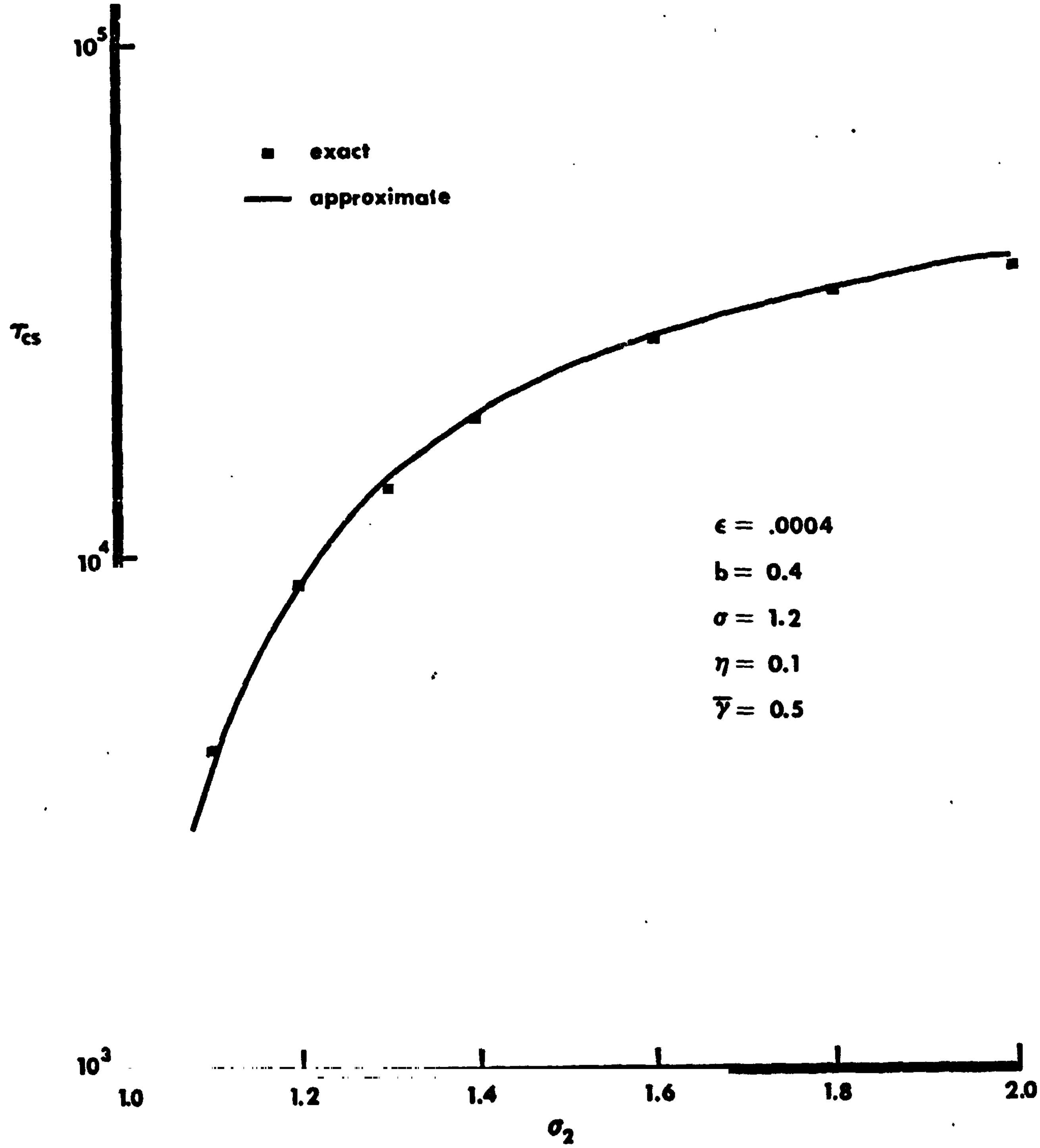

Figure 14 τ_{cs} vs. σ_2

was included in order to make the slug oscillate about $\beta=0$. The "exact" time constant was obtained by assuming exponential behavior for the maximum value of θ. From Figure 14 we see that the time constant given by (2.73) is a good approximation of the exact time constant even when $(\sigma_2-\sigma_1)$ is not small.

Nutation Synchronous Mode

When $\sigma_1 = \sigma_2$ the slug maintains a fixed position with respect to the nutation plane in the nutation synchronous mode. As the nutation angle slowly changes the position of the slug changes slowly. In the asymmetric case we would expect the behavior to be similar but in the asymmetric case θ oscillates. Thus for small oscillations in θ we would expect the slug to oscillate about some equilibrium point. For small oscillations of the slug the energy dissipation resulting from this oscillation would be small with respect to the total energy dissipation. The result should be a solution like the one for the symmetric case. However as $|\sigma_2-\sigma_1|$ increases or for large values of θ the magnitude of the oscillations in θ increases with the result that the energy dissipation from the oscillations of the slug could become significant. In this case we would expect a motion which is a combination of the nutation synchronous and spin synchronous modes of the symmetric case.

As in the symmetric case let α define the position of the slug with respect to the nutation plane.

$$\beta = \lambda\tau + \chi + \alpha \tag{2.76}$$

Substituting in (2.69) gives

$$\alpha'' + \eta\alpha' + \frac{\bar{I}_{uz}\omega_t}{2\sigma_1}\ [(\sigma_1\sigma_2+\sigma_2-\sigma_1)M^* + (\sigma_1\sigma_2+\sigma_1-\sigma_2)]\sin\alpha$$

$$+ [(\sigma_1\sigma_2+\sigma_1-\sigma_2)-(\sigma_1\sigma_2+\sigma_2-\sigma_1)M^*]\sin(2\lambda\tau+2\chi+\alpha) \quad = -\eta\lambda$$

where $M^* = \left(\frac{\sigma_1 - 1}{\sigma_2 - 1}\right)^{1/2}$

The coefficient of $\sin(2\lambda\tau + 2\chi + \alpha)$ is small compared to the coefficient of $\sin\alpha$, in fact it vanishes as for $\sigma_1 = \sigma_2$. An approximate solution for α obtained by the 1st iterate of a Picard iteration is

$$\alpha = \alpha_e + \frac{\bar{I}_{uz}\omega_t(\sigma_1\sigma_2+\sigma_2+\sigma_2-\sigma_1)(1-M^*)}{4\sigma_1\lambda(4\lambda^2+\eta^2)}[2\lambda\sin(2\lambda\tau+2\chi+\alpha_e)+\eta\cos(2\lambda\tau+2\chi+\alpha_e)] \quad (2.78)$$

where

$$\sin\alpha_e = \frac{-2\sigma_1\eta\lambda}{\omega_t[(\sigma_1\sigma_2+\sigma_2-\sigma_1)M^*+(\sigma_1\sigma_2+\sigma_1-\sigma_2)]} \quad (2.79)$$

Thus the magnitude of the oscillation is proportional to ω_t or θ and $|\sigma_2-\sigma_1|$. This oscillation in α will be neglected in determining the solution for ω_t. Substituting $\alpha = \alpha_e$ in (2.68) yields

$$\omega_t' = \epsilon\bar{\gamma}\ \frac{\bar{I}_{uz}(1+\lambda)^2}{2M^*}(1+M^*)\sin\alpha_e + \text{oscillatory terms} \quad (2.80)$$

The oscillatory terms contribute nothing to the decay of ω_t so they will be dropped. Substituting for $\sin\alpha_e$ gives

$$\omega_t\omega_t' = -\frac{\epsilon\bar{\gamma}\eta\lambda\sigma_1}{M^*} = -\epsilon\bar{\gamma}\eta(\sigma_2-1)$$

which has the solution

$$\omega_t = [\bar{\omega}_t^2 - 2\epsilon\bar{\gamma}\eta\sigma_1(\sigma_2-1)\tau]^{1/2} \tag{2.81}$$

Substituting into (2.67) the solution for θ becomes

$$\theta = \Big[|\sigma_1+\sigma_2-2|+|\sigma_2-\sigma_1|\cos 2(\lambda\tau+\chi)\Big]^{1/2} \frac{[\bar{\omega}_t^2-2\epsilon\bar{\gamma}\eta\sigma_1(\sigma_2-1)\tau]^{1/2}}{[2\sigma_1^2(\sigma_2-1)]^{1/2}} \tag{2.82}$$

Letting θ_o be the initial value of θ and assuming it is the maximum for the first oscillation we get

$$\theta = \left[\frac{|\sigma_1+\sigma_2-2|+|\sigma_2-\sigma_1|\cos 2(\lambda\tau+\chi)}{|\sigma_1+\sigma_2-2|+|\sigma_2-\sigma_1|}\right]^{1/2} (\theta_o^2-2\tau/\tau_{cn})^{1/2} \tag{2.83}$$

where

$$\tau_{cn} = \frac{2\sigma_1 \operatorname{sign}(\sigma_1+\sigma_2-2)}{\epsilon\bar{\gamma}\eta(|\sigma_1+\sigma_2-2|+|\sigma_2-\sigma_1|)} \tag{2.84}$$

A comparison of the damping constant τ_{cn} given by (2.84) and an "exact" τ_{cn} obtained by numerically integrating the exact equations of motion and assuming the maximum value of θ during each oscillation behaves according to

$$\theta_{max} = (\theta_o^2-2\tau/\tau_{cn})^{1/2}$$

is given in Figure 15. Figure 15 shows that the approximate solution developed is a good approximation even when $(\sigma_2-\sigma_1)$ is not small.

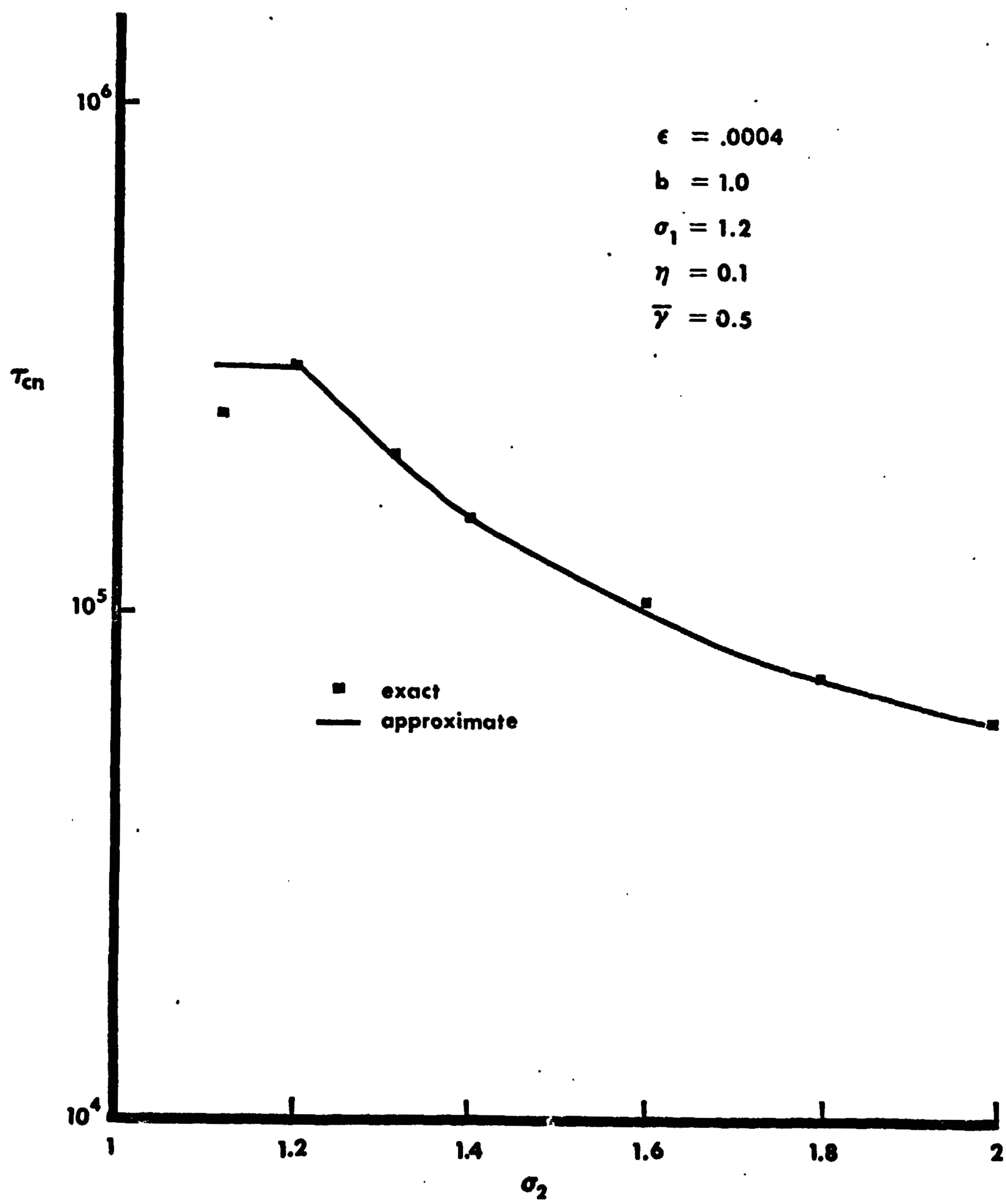

Figure 15 τ_{cn} vs. σ_2

3. Fluid Dynamics

In Section 2 approximate equations were developed for the nutation angle time history and the corresponding time constants. Comparison of these approximations with exact solutions obtained from numerical integration showed excellent agreement. However, this means that the comparison is good for the mathematical model of the system. Two important questions which still need to be answered are: 1) How good is the mathematical model? 2) If the mathematical model is valid how does one calculate the damping constant? The answer to both of these questions can come only from testing. In this section several methods for calculating the damping constant η for symmetric satellites are presented. The analysis of some test results is given in Section 4.

Nutation Synchronous Mode

In previous studies two approaches have been used to calculate the damping constant. Both approaches have drawbacks in that certain assymptions are made which are not completely valid. One approach is to model the motion of the fluid as steady flow in a pipe, and the other approach is to model it as boundary layer flow over a flat plate with the width of the plate being the perimeter of the pipe. Both of these approaches must be considered for both laminar and turbulent flow.

A) Steady Flow in a Pipe

1. Laminar Flow

The development of steady flow in a straight pipe can be found in almost any standard fluid mechanics text such as Reference 7.

Solution of the Navier-Stokes equations with a flux of

$$Q = \pi a^2 R\dot{\beta} \tag{3.1}$$

where $R\dot{\beta}$ is the velocity of the fluid slug relative to the ring and a is the radius of the ring, gives

$$u = 2R\dot{\beta}(1-(r/a)^2) \tag{3.2}$$

The shear stress at any point is

$$\tau = \mu\frac{\partial u}{\partial r} \tag{3.3}$$

where μ is the viscosity.
Thus the total viscous force is

$$F = (2\pi a)(R\gamma)\tau\Big|_{r=a} = 8\pi\mu R^2\dot{\beta}\gamma \tag{3.4}$$

Equating this to the force determined from the dynamic analysis, i.e.,

$$F = cv = cR\dot{\beta} = \eta m \Omega R \dot{\beta} \tag{3.5}$$

gives

$$\eta = 8\left(\frac{\bar{\nu}}{a^2\Omega}\right) \tag{3.6}$$

where $\bar{\nu}$ is the kinematic viscosity.
The quantity $\left(\frac{a^2\Omega}{\bar{\nu}}\right)$ is a Reynolds number but is not the standard Reynolds number for this type of analysis. The standard Reynolds number is

$$R_e = \frac{2aR\dot{\beta}}{\bar{\nu}} \tag{3.7}$$

Equation (3.6) holds for $R_e < 2000$ since the flow is laminar for $R_e < 2000$.

The analysis above assumed flow in a straight pipe but we have flow in a curved pipe. The correction factor for flow in a curved pipe as given by Schlicting[8] is

$$\tau/\tau_o = 0.1064[R_e(a/R)^{1/2}]^{1/2} \qquad (3.8)$$

where τ_o is the shear stress in the straight pipe and τ is the shear stress in the curved pipe. Equation (3.8) is valid for $10^{1.6} < (a/R)^{1/2}R_e < 10^3$. For $R_e = 2000$ and $(a/R) = 1/100$ the increase in shear stress is 50%. Therefore one should take into account the curvature of the pipe. Thus for laminar flow the damping constant becomes

$$\eta = 1.2(\frac{\bar{\nu}}{a^2\Omega})^{1/2}(\frac{R}{a})^{1/4}|\sigma-1|^{1/2} \qquad (3.9)$$

The assumption here is that we have steady flow in a pipe but a certain length is required for steady flow to develop. For flow from a cistern into a pipe this length (Ref. 8 pg. 301) is

$$\delta = 0.0575\, a R_e \qquad (3.10)$$

which for $R_e = 1500$ is $\delta = 86a$. But the length of the fluid in many cases may not be much more than 86a. Thus the length of fluid required for steady flow to develop may be about equal to the length of the fluid. Thus there is an error in assuming steady flow.

2. Turbulent Flow

Blasius (Ref. 8 pg. 339) developed for the shear stress for steady turbulent flow in a straight pipe the empirical result

$$\tau = 0.0791\, R_e^{-1/4}(\frac{1}{2}\rho u_m^2) \qquad (3.11)$$

where u_m is the mean velocity $R\dot{\theta}$. This result is valid for $R_e < 10^5$. Using the same procedure as before to calculate the damping constant one obtains

$$\eta = 0.133\left(\frac{\bar{\nu}}{a^2\Omega}\right)^{1/4}\left(\frac{R}{a}\right)^{3/4}|\sigma-1|^{3/4} \tag{3.12}$$

The correction factor to take into account the fact that the flow is in a curved pipe is

$$\tau/\tau_o = 1. + 0.075\, R_e^{1/4}(a/R)^{1/2} \tag{3.13}$$

The correction factor for turbulent flow is smaller than that for laminar flow and can be neglected since it is usually less than 10%. With the correction factor the damping constant becomes

$$\eta = 0.133\left(\frac{\bar{\nu}}{a^2\Omega}\right)^{1/4}\left(\frac{R}{a}\right)^{3/4}|\sigma-1|^{3/4}\left[1+0.089\left(\frac{a^2\Omega}{\bar{\nu}}\right)^{1/4}\left(\frac{a}{R}\right)^{1/4}|\sigma-1|^{1/4}\right] \tag{3.14}$$

If the fluid is free from disturbances at entry the flow in a smooth pipe for some distance δ from the entry will be laminar even though turbulence develops further downstream. The Reynolds number at which the transition occurs may be expected to have the same order of magnitude as the Reynolds number for transition in flow along a flat plate. When the conditions are disturbed at entry the distance required for the velocity to take its final form is less but it depends on the amount of disturbance. When the flow is fully turbulent the inlet length δ has been found to be

$$\delta = 1.386\, a R_e^{1/4} \tag{3.15}$$

which for $R_e = 10^4$ is $\delta = 13.86$ which is considerably less than that for laminar flow. Thus the error which results from the assumption of steady flow in a pipe is less in the turbulent region than in the laminar region.

B) Flow Past a Flat Plate

1. Laminar Flow

Since the flow for some distance from the cntry is similar to boundary layer flow past a flat plate a reasonable assumption is to treat the problem as boundary layer flow as was done by Carrier and Miles[1,2]. The drag force on a flat plate of width b and length ℓ is

$$D = 0.664\, b\ell^{1/2}\rho\bar{\nu}^{1/2}U_\infty^{3/2} \tag{3.16}$$

From the dynamic analysis

$$D = c_d U_\infty = c_d R\dot{\beta} = \eta m \Omega R\dot{\beta} \tag{3.17}$$

The damping constant η becomes

$$\eta = 1.328\left(\frac{\bar{\nu}}{a^2\Omega}\right)^{1/2} \frac{|\sigma-1|^{1/2}}{\gamma^{1/2}} \tag{3.18}$$

The question which now must be asked is: What it the distance or length required for the boundary layer to disappear? Defining the boundary layer thickness ϵ as the distance for which $u = 0.99\, U_\infty$ then (Schlicting,[8] pg. 122)

$$\epsilon \approx 5\frac{\sqrt{\nu\delta}}{U_\infty} \tag{3.19}$$

Setting ϵ equal to the radius of the pipe yields

$$\delta = \left(\frac{R_e}{25}\right)a \tag{3.20}$$

which may or may not be a substantial portion of the fluid slug. Thus in the laminar region neither the steady flow in a pipe approach or the boundary layer approach may be a good approximation since neither is valid for the entire length of the fluid.

2. Turbulent Flow

The drag force on a flat plate of width b and length ℓ when the boundary layer is turbulent is (see Schlicting,[8] pg. 536).

$$D = 0.037 \rho U_\infty^2 b \ell \left(\frac{U_\infty \ell}{\bar{\nu}}\right)^{-1/5} \tag{3.21}$$

Equating this to the viscous drag force

$$D = c_d U_\infty = c_d R \dot{\beta} \qquad \eta m \Omega R \dot{\beta}$$

one obtains

$$\eta = 0.074 \left(\frac{\bar{\nu}}{a^2 \Omega}\right)^{1/5} \left(\frac{R}{a}\right)^{3/5} \gamma^{-1/5} |\sigma - 1|^{4/5} \tag{3.22}$$

This equation is valid for

$$5 \times 10^5 < \left(\frac{R\gamma}{2a}\right) R_e < 10^7 \tag{3.23}$$

Spin Synchronous Mode

In this mode the velocity of the fluid is not constant but oscillatory with respect to the ring. An approach suggested by Leibold[6] to obtain a damping constant is to use the results of Bhuta and Koval[10], who analyzed the nutation damping of a satellite with a completely filled viscous ring damper mounted on a plane parallel to the spin axis. They modelled the motion of the fluid as a fluid in an infinite pipe with the pipe executing harmonic motion, and then obtained the energy dissipation rate which leads to the damping constant.

To apply their analysis to this problem it is assumed that the analysis is valid for a finite length of fluid, the energy dissipation rate is then averaged over m cycles to determine the average rate of energy dissipation. This average rate is then used to calculate the damping constant. From Bhuta and Koval the energy dissipation/unit-length at the end of the m^{th} cycle is

$$E = \frac{2U^2\mu\pi}{s}\sum_{n=1}^{\infty}\frac{r_n^6}{(r_n^4+\zeta^2)^2}\left[\exp\left(\frac{-4r_n^2 m\pi}{\zeta}\right)-1\right]+\frac{U^2\mu m\pi^2}{s}i\{\sqrt{i\zeta}\,I_0\bar{I}_1-\sqrt{-i\zeta}\,\bar{I}_0 I_1\}/I_0\bar{I}_0 \tag{3.24}$$

where I_0 and I_1 are modified Bessel functions of the first kind and

$$I_j = I_j(\sqrt{i\zeta})$$

$$\bar{I}_j = I_j(\sqrt{-i\zeta}) \tag{3.25}$$

$$\zeta = \frac{sa^2}{\bar{\nu}}$$

U is the maximum velocity of the tube with respect to the fluid, a is the radius of the tube, s is the excitation frequency and the r_n are the zeros of $J_o(r_n)$. Letting $g(\zeta)$ be the average amount of energy dissipation/cycle/unitmass/vel.^{2} one obtains for the damping constant

$$\eta = \frac{|\lambda|}{\pi}g(\zeta) \tag{3.26}$$

where

$$g(\zeta) = \frac{\pi}{\zeta}i\left(\frac{\sqrt{i\zeta}\,I_0\bar{I}_1-\sqrt{-i\zeta}\,\bar{I}_0 I_1}{I_0\bar{I}_0}\right)+\frac{2}{m}\sum_{n=1}^{\infty}\frac{r_n^6}{(r_n^4+\zeta^2)^2}\left[\exp\left(-\frac{4r_n^2 m\pi}{\zeta}\right)-1\right] \tag{3.27}$$

$g(\zeta)$ is plotted for several values of m in Figure 16. Since $g(\zeta)$ for $m > 20$ and $g(\zeta)$ for $m = \infty$ are approximately equal, it is reasonable to just use the value of $g(\zeta)$ when $m = \infty$ which is

$$g(\zeta) = \frac{\pi i}{\zeta}\left(\frac{\sqrt{i\zeta}\; I_0\bar{I}_1 - \sqrt{-i\zeta}\; \bar{I}_0 I_1}{I_0\bar{I}_0}\right) \tag{3.28}$$

The excitation frequency s is

$$s = |\sigma - 1|\Omega \quad .$$

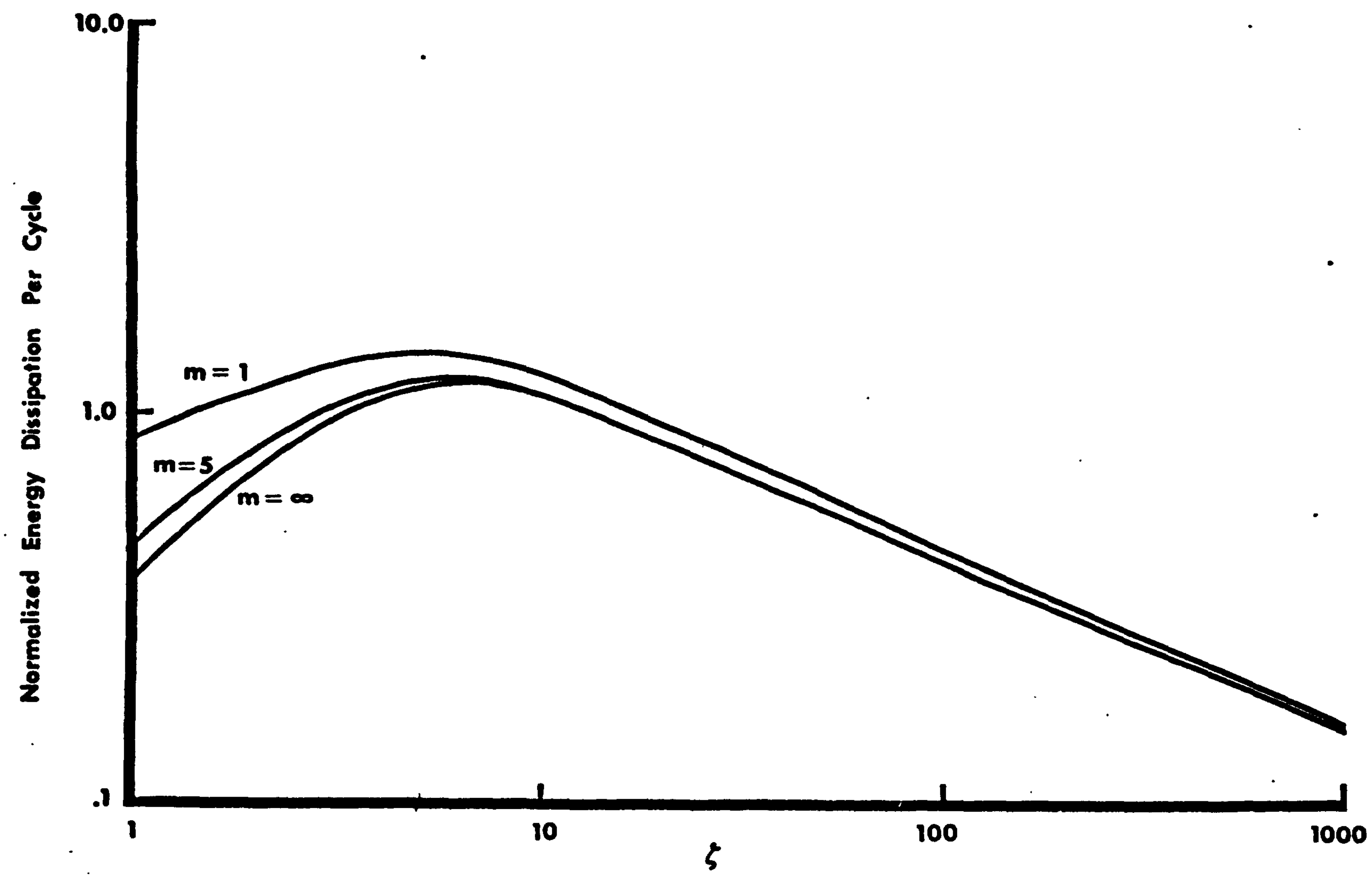

Figure 16 Normalized Energy Dissipation Per Cycle vs. ζ

4. Test Data Analysis

In October 1972 a series of tests were run at NASA/GSFC on the Helios damper. A total of 36 tests were run with four inertia ratios (0.337, 0.50, 0.51, 1.126) and two damper locations (30 in. and 9 in. above the satellite center of mass). In all of the tests the damper was offset 0.25 in. from the spin axis. The test results and parameters as reported by Hraster[11] are reproduced in Tables 4.1 and 4.2.

In each series of tests the satellite was balanced with the empty ring attached. Therefore, during the tests one could consider that gravity is acting only on the slug. With this assumption the effect of gravity on the nutational behavior of the satellite was determined in Section 2.3.

In analyzing the test data the first thing which must be determined is in which mode, the nutation synchronous or spin synchronous, the satellite is operating. Because of the offset of the damper axis it is reasonable to assume the fluid is behaving like a rigid slug. In all of the tests the nutation angle time history appears to have an exponential behavior, hence it is assumed the satellite was in the spin synchronous mode. Using the development of Section 2 the effect of gravity on the time constant was removed and using Equation (2.30) a value of the damping constant η and the transition angle θ_T were calculated. These results are given in Table 4.3. Note that the time constant for zero gravity decreases with spin speed but the time constant for the tests increased with spin speed. Those tests for which there is no entry in the η column there was no value of η which would give time constant. However, for all of those except the last series of tests a 10% change in the time constant would give a reasonable value of η.

Table 4.1

SEQ. NO.	RPM	t_c(sec)	θ_{max}(deg)
0.5	33.3	107	2.35
0.51	31.1	105	2.35
1.0	63.7	2049	.5
1.1	61.3	994	1.5
2.0	81.5	1945	1.
2.1	79.8	2208	.62
3.0	102.3	1900	1.2
3.1	103	2398	1.6
4.0	123.2	1738	.25
4.1	124.4	2769	1.5
c/o	31.1	76.7	3.5
5.0	61.6	383	.62
5.1	60.9	388	1.2
5.2a	60.4	376	1.4
5.2b	60.4	296	2.2
5.2c	60.4	295	4.7
6.0	85.5	554	1.6
6.1	81.2	574	.75
7.0	101.8	816	.75
7.1	102.2	624	1.1
8.0	119.5	1256	.12
8.1	119.5	803	.37
c/o	31.5	118	2.5
9.0	62.7	879	.88
9.1	61.7	834	.5
10.0	82.1	1302	.62
11.0	102.1	1468	.62
11.1	99.7	1390	.5
12.0	120.0	2032	.31
17.0	62.3	155.9	very small
17.1	62.3	191.6	" "
18.0	81.1	19.1	" "
18.1	81.2	20.9	" "
19.0	103.1	13.2	" "
19.1	102.6	11.5	" "
20.0	120	7.8	" "
20.1	120.8	10.25	" "

Table 4.2

$m = 0.152$ kg.

$R = 29$ cm. $\quad a = 0.28$ cm.

$\bar{\gamma} = 0.25 \quad \gamma = \pi/2$

$\nu = 1.17 \times 10^{-3} cm^2/sec$

SEQ. NO.	A(slug-ft^2)	σ	b=h/R	ϵ
0.50-4.1	59.37	0.337	2.63	6.35×10^{-4}
5.00-8.1	65.85	0.500	2.63	5.72×10^{-4}
9.00-12.0	65.85	0.510	0.788	5.72×10^{-4}
17.00-20.1	40.05	1.126	0.788	9.42×10^{-4}

Table 4.3

SEQ.NO.	RPM	t_c	$t_c(g=0)$	η	θ_T(deg)	G^2
0.50	33.3	107	11,400	-	-	106.7
0.51	31.1	105	14,350	-	-	136.9
1.0	63.7	2049	25,800	.102	4.1	12.6
1.1	61.3	996	14,000	.209	7.8	14.1
2.0	81.5	1945	12,700	.168	9.2	6.54
2.1	79.8	2208	15,200	.141	7.6	6.89
3.0	102.3	1900	7,520	.241	16.6	3.96
3.1	103.	2398	9,300	.183	12.9	3.90
4.0	123.2	1738	4,920	.342	26.6	2.83
4.1	124.4	2769	7,700	.184	15.2	2.78
c/o	31.1	76.7	2,630	-	-	34.3
5.0	61.6	383	1,945	.254	5.4	5.01
5.1	60.9	388	1,995	.243	5.2	5.14
5.2a	60.4	376	1,970	.251	5.3	5.24
5.2b	60.4	296	1,550	-	-	5.24
5.2c	60.4	295	1,550	-	-	5.24
6.0	85.5	554	1,490	.224	6.6	2.7
6.1	81.2	574	1,680	.203	5.7	2.93
7.0	101.8	816	1,720	.148	4.9	2.11
7.1	102.2	624	1,310	.209	6.9	2.10
8.0	119.5	1256	2,220	.093	3.4	1.77
8.1	119.5	803	1,420	.154	5.6	1.77
c/o	31.5	118	30,900	.419	3.9	262.
9.0	62.7	379	20,500	.220	6.9	23.4
9.1	61.7	834	20,500	.226	6.9	24.6
10.0	82.1	1302	13,700	.279	12.9	10.5
11.0	102.1	1468	8,780	-	-	5.99
11.1	99.7	1390	8,800	-	-	6.34
12.0	120.0	2032	8,500	.345	24.1	4.19
17.0	62.3	155.9	505.2	-	-	3.24
17.1	62.3	191.6	620.8	-	-	3.24
18.0	81.1	19.1	41.3	-	-	2.16
18.1	81.2	20.9	45.1	-	-	2.16
19.0	103.1	13.2	21.9	-	-	1.66
19.1	102.6	11.5	19.1	-	-	1.66
20.0	120.0	7.8	11.4	-	-	1.46
20.1	120.8	10.25	15.0	-	-	1.46

Using the analysis of Section 3 a value of η has been determined for each test and the calculations are presented in Table 4.4. Table 4.4 shows that the value of η calculated from the data is 4 to 5 times larger than the predicted value. It was originally thought that this difference was probably due to the offset but investigation has shown that the offset has very little effect on the time constant. Several possible reasons for this difference between the predicted and actual values of η are: 1) the method of calculating η in Section 3 is not valid, 2) the effect of gravity on the tests, 3) the mathematical model of the fluid behaving as a rigid slug in the spin synchronous mode, or 4) some combination of the above.

In the forth series of tests no value of the damping constant could be evaluated. It was originally thought that this was due to the offset since the offset angle is 1.5 deg. and the nutation angle was less than 0.1 degrees. For nutation angles this small the offset did cause a decrease of about 25% in the time constant but this is not enough to explain the test results. Another contributing factor is that the nutation angles were so small that measurement of the time constant was difficult.

For the first two series of tests the time constant has been scaled to the Helios satellite and is given in Table 4.5. A value of $\eta = 0.174$ was obtained by averaging the test data for $\Omega = 95$ rpm. The corresponding time constant was then calculated.

Since there is no test data for motion in the nutation synchronous mode there can be no comparison between actual and predicted time constants for that mode.

Table 4.4

SEQ.NO.	η(test data)	η(pred)
0.50	-	.0720
0.51	-	.0742
1.0	.102	.0541
1.1	.209	.0550
2.0	.168	.0485
2.1	.141	.0490
3.0	.241	.0440
3.1	.183	.0438
4.0	.342	.0404
4.1	.184	.0403
4.0	-	.0633
5.0	.254	.0469
5.1	.243	.0471
5.2a	.251	.0473
5.2b	-	.0473
5.2c	-	.0473
6.0	.224	.0406
6.1	.203	.0415
7.0	.148	.0376
7.1	.209	.0375
8.0	.093	.0350
8.1	.154	.0350
c/o	.419	.0623
9.0	.220	.0460
9.1	.226	.0463
10.0	.279	.0408
11.0	-	.0371
11.1	-	.0375
12.0	.345	.0346
17.0	-	.0216
17.1	-	.0216
18.0	-	.0192
18.1	-	.0192
19.0	-	.0173
19.1	-	.0173
20.0	-	.0162
20.1	-	.0162

Table 4.5

	Test 1		
	Helios	A/B	A/B
I_T(SLUG-FT^2)	332.2	59.37	65.85
$I_S/I_T = \sigma$	0.385	0.337	0.50
h(IN)	30.23	30.0	30.0
ω(RPM)	95	95	95
η (damping const)	0.174	0.174	0.17
t_c (flight condition) sec	48,500.	10,350.	1,542.

5. Summary

A ring which is partially filled with a viscous fluid has been analyzed as a nutation damper for a spinning satellite. Since it was shown by Carrier and Miles[1,2] that the fluid behaves as a rigid slug for very small mutation angles the fluid has been modelled as a rigid slug of finite length resisted by a linear viscous force. With these assumptions it has been shown that there are two distinct modes of motion, the nutation synchronous mode and the spin synchronous mode.[3,4] For the symmetric satellite in the spin synchronous mode the mutation angle exhibits exponential behavior plus a small oscillation with the exponential portion given by

$$\theta = \theta_o e^{-\tau/\tau_{cs}} \tag{5.1}$$

where

$$\tau_{cs} = \frac{2(\sigma-1)[(\sigma-1)^2+\eta^2]}{\epsilon\bar{\gamma}\eta b^2 k^2 \sigma^3} \tag{5.2}$$

In the mutation synchronous mode the cosine of the mutation angle exhibits exponential behavior

$$\cos\theta = \cos\theta_o e^{\tau/\tau_{cn}} \tag{5.3}$$

$$\tau_{cn} = \frac{\sigma}{\epsilon\bar{\gamma}\eta(\sigma-1)} \tag{5.4}$$

For small angles (5.3) becomes

$$\theta = \left(\theta_o^2 - \frac{2\tau}{\tau_{cn}}\right)^{1/2} \tag{5.5}$$

The transition angle between the two modes is given by

$$\tan\theta_T = \frac{\eta(\sigma-1)}{b\sigma^2 k} \tag{5.6}$$

Comparisons of τ_{cs} and τ_{cn} with "exact" time constants obtained from numerical integration of the equations of motion are given in Figures 3-12. The agreement is good.

The damper was then analyzed for the asymmetric case and it was found that the two modes still exist. For the spin synchronous mode

$$\frac{1}{\tau_{cs}} = \frac{\epsilon\bar{\gamma}\eta b^2 k^2}{2\sigma_1[(\sigma_1-1)(\sigma_2-1)+\eta^2]}\left[\frac{(\sigma_1\sigma_2+\sigma_2-\sigma_1)}{(\sigma_2-1)}\cos^2\beta_o+\frac{(\sigma_1\sigma_2+\sigma_1-\sigma_2)}{(\sigma_1-1)}\sin^2\beta_o\right] \tag{5.7}$$

In the spin synchronous mode the slug oscillates in the tube while moving slowly around the tube. In (5.7) β_o is the position about which the slug is oscillating. Since β_o changes slowly with time τ_{cs} is a slowly varying function of time, it oscillates between the two values of τ_{cs} obtained by setting $\beta_o = 0$ and $\beta_o = \pi/2$. For a design criteria one should use the maximum value of τ_{cs}.

In the nutation synchronous mode for the asymmetric satellite we have

$$\theta = \left[\frac{|\sigma_1+\sigma_2-2|+|\sigma_2-\sigma_1|\cos 2\lambda\tau}{|\sigma_1+\sigma_2-2|+|\sigma_2-\sigma_1|}\right]^{1/2}\left(\theta_o^2-\frac{2\tau}{\tau_{cn}}\right)^{1/2} \tag{5.8}$$

$$\tau_{cn} = \frac{2\sigma_1\,\mathrm{sign}(\sigma_1+\sigma_2-2)}{\epsilon\bar{\gamma}\eta(|\sigma_1+\sigma_2-2|+|\sigma_2-\sigma_1|)} \tag{5.9}$$

The equation for θ is valid only for small nutation angles whereas the results for the nutation synchronous mode in the symmetric case are valid for all nutation angles. Comparisons of τ_{cs} and τ_{cn} given by (5.7) and (5.9) with "exact" time constants are given in Figures 14 and 15.

The effect of an offset of the center of the ring from the spin axis was investigated and was found to have only a very small effect on τ_{cs} and τ_{cn}.

For a symmetric satellite an investigation was made of the effect of a stop in the tube. Since the behavior of the fluid when it encounters a stop in the tube is not known a very simple mathematical model was used. The results show that the stop increases the amount of energy dissipation but no analytical result was obtained to predict the increase in energy dissipation. Some results are given in Section 2.4.

Since τ_{cn} and τ_{cs} are a function of the damping constant η a method of calculating η is needed. In Section 3 several methods of calculating η are developed from a consideration of the fluid dynamics.

Analysis of the test results obtained from tests performed at NASA/GSFC on the Helios satellite is given in Section 4. Before analyzing the results it was necessary to determine the effect of gravity on the behavior of the system. For the symmetric satellite it was found that gravity does not effect τ_{cn} but

$$\tau_{cs}(\text{test}) = \frac{\tau_{cs}(\text{no gravity})}{G^2} \tag{5.10}$$

where

$$G = \left(1 + \frac{\bar{g}}{\sigma^2 b}\right) \tag{5.11}$$

$\bar{g}$ is the ratio of the gravitational force to the centrifugal force which is the inverse of the Froude number.

$$\bar{g} = g/R\Omega^2 \tag{5.12}$$

Thus gravity can have a substantial effect on the test results.

The test results show that during the tests all motion was in the spin synchronous mode. Thus no comparison can be made with the theoretical results for the nutation synchronous mode. The theoretical damping constant η developed in Section 3 was off by a factor of approximately 4 or 5 from the value of η calculated from the test results.

References

1. Carrier, G.F. and Miles, J.W., "On the Annular Damper for a Freely Precessing Gyroscope", J. of Applied Mechanics, June 1960, pp. 237-240.

2. Miles, J.W., "On the Annular Damper for a Freely Precessing Gyroscope-II", J. of Applied Mechanics, June 1963, pp. 189-192.

3. Cartwright, W.F., Massingill, E.C., and Trueblood, R.D., "Circular Constraint Nutation Damper", AIAA J., vol. 1, No. 6, June 1963, pp. 1375-1380.

4. Carwright, W.F., Massingill, E.C. and Trueblood, R.D., Circular Constraint Nutation Damper Analysis, GM DRL Dept. TM 62-205, General Motors Corp., 1961.

5. Alfriend, K.T., Analysis of a Partially Filled Viscous Ring Damper, NASA TM X-732-71-456, October 1971.

6. Leibold, G., Nutational Behavior of the Helios-Planetcid Together with the MBB Liquid Nutation Damper, Project Helios, Doc. No. 2-4440-011-00, Feb. 1972.

7. Modern Developments in Fluid Dynamics, ed. by S. Goldstein, 1938.

8. Schli ting, H., Boundary Layer Theory, McGraw Hill, 1960.

9. Bhuta, P.G. and Koval, L.R., "A Viscous Ring Damper for a Freely Precessing Satellite", Int. J. of Mech. Sciences, vol. 8, 1966, pp. 383-395.

10. Salvatore, J.O. and Porter, W.W., ATS-V Heat Pipe Tests and Dimensional Analysis, Hughes Ref. No. C2325, Hughes Aircraft Co., June 1970.

11. Hraster, J.A., Memorandum to H.C. Hoffman, 20 November 1972.

Appendix A

Equations of Motion

The system is assumed to consist of an asymmetric rigid body (the satellite) and a circular tube of radius R which is attached to the rigid body at a distance h along the spin axis from the center of mass. The center of the ring is offset a distance δ from the spin axis. Moving in the tube is a rigid slug which fills a portion of the tube, the fraction fill being $\bar{\gamma}$. The only other assumptions are: 1) the center of mass of the system and the center of mass of the satellite are coincident, 2) the motion of the slug is resisted by a linear viscous force, and 3) gravity acts only on the slug (the satellite is statically balanced).

Referring to Figure 1 the x, y and z axes are principal axes of the satellite and z is the spin axis. The u, v, z system rotates about the z-axis relative to the x, y, z system such that the u axis passes through the center of mass of the slug. Using the u, v, z coordinate system the equations of motion are obtained by equating the time rate of change of the angular momentum to the external moments and using Lagrange's equation for the motion of the rigid slug in the tube. The angular momentum of the system about the satellite center of mass is

$$\begin{aligned}
\underset{\sim}{H} = {} & \left\{\left[\frac{(A+B)}{2} + \frac{(A-B)}{2}\cos 2\beta + I^*_{uu}\right]\omega_u - \left[\frac{(A-B)}{2}\sin 2\beta + I^*_{uv}\right]\omega_v - I^*_{uz}(\omega_z + \dot{\beta})\right\}\underset{\sim}{e}_u \\
& + \left\{-\left[\frac{(A-B)}{2}\sin 2\beta + I^*_{uv}\right]\omega_u + \left[\frac{(A+B)}{2} - \frac{(A-B)}{2}\cos 2\beta + I^*_{vv}\right]\omega_v - I^*_{vz}(\omega_z + \beta')\right\}\underset{\sim}{e}_v \qquad \text{(A1)} \\
& + \left\{-I^*_{uz}\omega_u - I^*_{vz}\omega_v + C\omega_z + I^*_{zz}(\omega_z + \dot{\beta})\right\}\underset{\sim}{e}_z
\end{aligned}$$

where A, B and C are the principal moments of inertia of the satellite and the $I^*_{\alpha\beta}$ are the moments and products of inertia of the slug about the satellite center of mass. The $I_{\alpha\beta}$ are given in Appendix B.

The gravitational force is

$$\underset{\sim}{F} = -mg\,\underset{\sim}{N}_z = -mg[\sin\theta\sin(\psi+\beta)\underset{\sim}{e}_u+\sin\theta\cos(\psi+\beta)\underset{\sim}{e}_v+\cos\theta\underset{\sim}{e}_z] \qquad \text{(A2)}$$

where θ, ψ and ϕ are the Euler angles of the satellite. The radius vector to the slug center of mass is

$$\underset{\sim}{r}_c = [Rk+\delta\cos(\beta-\nu)]\underset{\sim}{e}_u - \delta\sin(\beta-\nu)\underset{\sim}{e}_v + h\underset{\sim}{e}_z \qquad \text{(A3)}$$

where

$$k = \frac{\sin(\gamma/2)}{(\gamma/2)} \qquad \text{(A4)}$$

The moment due to gravity becomes

$$\begin{aligned}\underset{\sim}{M} = -mg\Big\{&[-\delta\sin(\beta-\nu)\cos\theta-h\sin\theta\cos(\psi+\beta)]\underset{\sim}{e}_u\\ &+[h\sin\theta\sin(\psi+\beta)-(Rk+\delta\cos(\beta-\nu))\cos\theta]\underset{\sim}{e}_v \qquad \text{(A5)}\\ &+[(Rk+\delta\cos(\beta-\nu))\sin\theta\cos(\psi+\beta)+\delta\sin(\beta-\nu)\sin\theta\sin(\psi+\beta)]\underset{\sim}{e}_z\Big\}\end{aligned}$$

The kinetic energy of the fluid slug is

$$T_{FS} = \frac{1}{2}m v_c^2 + \frac{1}{2}\underset{\sim}{H}_c\cdot\underset{\sim}{\omega} = \underset{\sim}{H}_{FS} + \frac{1}{2}m v_{cr}^2 + m\underset{\sim}{v}_{cr}\cdot(\underset{\sim}{\omega}\times\underset{\sim}{r}_c) \qquad \text{(A6)}$$

where $\underset{\sim}{v}_c$ is the velocity of the center of mass of the slug, $\underset{\sim}{v}_{cr}$ is the velocity of the center of mass of the slug relative to a coordinate system whose origin is at the satellite center of mass and whose axes are parallel to the u, v, z axes, $\underset{\sim}{\omega}$ is the angular velocity of the fluid slug and $\underset{\sim}{H}_{FS}$ is the angular momentum of the slug. Using (A3)

$$\underset{\sim}{v}_{cr} = -\delta\dot{\beta}[\sin(\beta-\nu)\underset{\sim}{e}_u+\cos(\beta-\nu)\underset{\sim}{e}_v] \tag{A7}$$

The kinetic energy becomes

$$T_{FS} = \frac{1}{2}[I^*_{uu}\omega_u^2+I^*_{vv}\omega_v^2+I^*_{zz}(\omega_z+\dot{\beta})^2-2I^*_{uv}\omega_u\omega_v-2I^*_{uz}\omega_u(\omega_z+\dot{\beta})-2I^*_{vz}\omega_v(\omega_z+\dot{\beta})]$$
$$-m\delta\dot{\beta}[h(\omega_v\sin(\beta-\nu)-\omega_u\cos(\beta-\nu))+Rk(\omega_z+\dot{\beta})\cos(\beta-\nu)+\delta(\omega_z+\dot{\beta}/2)] \tag{A8}$$

The potential energy is

$$V = mg\, \underset{\sim}{r}_c\cdot\underset{\sim}{N}_z$$

$$V = mg\, Rk\, \sin\theta\sin(\psi+\beta)+\delta\sin\theta\sin(\psi-\nu)+h\, \cos\theta] \tag{A9}$$

The generalized force due to the line iscous force is

$$Q_\beta = -c_d R^2\dot{\beta} \tag{A10}$$

In the development of the approximate solutions it is advantageous to use dimensionless variables and constants. The angular rates and time are made dimensionless using Ω, the initial spin rate. Let

$$\tau = \Omega t \tag{A11}$$

$$\omega_u = \Omega p$$
$$\omega_v = \Omega q \tag{A12}$$
$$\omega_z = \Omega r$$

A suitable set of dimensionless parameters are

$$
\begin{aligned}
\sigma_1 &= C/A \\
\sigma_2 &= C/B \\
b &= h/R \\
\bar{\delta} &= \delta/R \\
\eta &= c_d/m\Omega \\
\epsilon &= \frac{mR^2}{A\bar{\gamma}} \\
\bar{g} &= \frac{g}{R\Omega^2}
\end{aligned}
\tag{A13}
$$

In addition to these we have $\bar{\gamma}$, the fraction fill, and ν. ϵ is a small parameter which is the ratio of the moment of inertia of the tube filled with fluid to one of the transverse moments of inertia of the satellite. It was chosen in this manner so that ϵ would remain constant when varying γ or $\bar{\gamma}$. η is a dimensionless damping parameter. $\bar{g}$ measures the effect of gravity and is actually the inverse of the Froude number. Substituting (A11)-(A13) into (A1), (A5), (A8), (A9) and (A10) gives

$$\frac{\underset{\sim}{H}}{A\Omega} = \left\{ \left[\frac{(1+\sigma_{12})}{2} + \frac{(1-\sigma_{12})}{2}\cos 2\beta\right]p - \left[\frac{(1-\sigma_{12})}{2}\sin 2\beta\right]q \right.$$

$$\left. + \left[I_{uu}p - I_{uv}q - I_{uv}(r+\beta')\right] \right\} \underset{\sim}{e}_u$$

$$+ \left\{ -\left[\frac{(1-\sigma_{12})}{2}\sin 2\beta\right]p + \left[\frac{(1+\sigma_{12})}{2} - \frac{(1-\sigma_{12})}{2}\cos 2\beta\right]q \right. \qquad \text{(A14)}$$

$$\left. + \left[-I_{uv}p + I_{vv}q - I_{vz}(r+\beta')\right] \right\} \underset{\sim}{e}_v$$

$$+ \left\{ \sigma_1 r + \left[-I_{uz}p - I_{vz}q + I_{zz}(r+\beta')\right] \right\} \underset{\sim}{e}_z \quad .$$

where

$$\sigma_{12} = \sigma_1/\sigma_2 \qquad \text{(A15)}$$

$$(\ )' = \frac{d}{d\tau} \qquad \text{(A16)}$$

$$\frac{\underset{\sim}{M}}{A\Omega^2} = -\epsilon\bar{\gamma}\bar{g} \left\{ \left[-\bar{\delta}\sin(\beta-\nu)\cos\theta - b\ \sin\theta\cos(\psi+\beta)\right]\underset{\sim}{e}_u \right.$$

$$+ \left[b\ \sin\theta\sin(\psi+\beta) - (k+\bar{\delta}\cos(\beta-\nu))\cos\theta\right]\underset{\sim}{e}_v \qquad \text{(A17)}$$

$$\left. + \left[(k+\bar{\delta}\cos(\beta-\nu))\sin\theta\cos(\psi+\beta) + \bar{\delta}\sin(\beta-\nu)\sin\theta\sin(\psi+\beta)\right]\underset{\sim}{e}_z \right\}$$

$$\frac{T_{F3}}{mR^2\Omega^2} = \frac{1}{2}\left[\bar{I}_{uu}p^2 + \bar{I}_{vv}q^2 + \bar{I}_{zz}(r+\beta')^2 - 2\bar{I}_{uv}pq - 2\bar{I}_{uz}p(r+\beta') - 2\bar{I}_{vz}q(r+\beta')\right] \qquad \text{(A18)}$$

$$-\bar{\delta}\beta'\left[b(q\ \sin(\beta-\nu) - p\ \cos(\beta-\nu)) + k(r+\beta')\cos(\beta-\nu) + \bar{\delta}(r+\beta'/2)\right]$$

$$\frac{V}{mR^2\Omega^2} = \bar{g}\left[k\ \sin\theta\sin(\psi+\beta) + \sin\theta\sin(\psi-\nu) + b\ \cos\theta\right] \qquad \text{(A19)}$$

$$\frac{Q_\beta}{mR^2\Omega^2} = -\eta\beta' \qquad \text{(A20)}$$

Applying

$$\frac{d\underset{\sim}{H}}{dt} = \underset{\sim}{M} \tag{A21}$$

and

$$\frac{d}{dt}\frac{\partial T}{\partial \dot{\beta}} - \frac{\partial T}{\partial \beta} = Q_\beta - \frac{\partial V}{\partial \beta} \tag{A22}$$

and noting that

$$\frac{\partial T}{\partial \beta} = \left.\frac{\partial T}{\partial \beta}\right|_{p,q\,=\,\text{const}} + q\frac{\partial T}{\partial p} - p\frac{\partial T}{\partial q} \tag{A23}$$

since p and q depend implicitly on β via

$$\begin{aligned} \omega_u &= \omega_x \cos\beta + \omega_y \sin\beta \\ \omega_v &= -\omega_x \sin\beta + \omega_y \cos\beta \end{aligned} \tag{A24}$$

the equations of motion become

$$\begin{aligned} &\left[\frac{(1+\sigma_{12})}{2} + \frac{(1-\sigma_{12})}{2}\cos 2\beta + I_{uu}\right]p' + \left[-\frac{(1-\sigma_{12})}{2}\sin 2\beta - I_{uv}\right]q' \\ &-I_{uz}(r'+\beta'') = [-I'_{uu}+(1-\sigma_{12})\sin 2\beta]p\beta' + [I'_{uv}+(1-\sigma_{12})\cos 2\beta]q\beta' \\ &+ I'_{uz}(r+\beta')\beta' + (r+\beta')\bar{H}_v - q\bar{H}_z + \bar{M}_u \end{aligned} \tag{A25}$$

$$[-\frac{(1-\sigma_{12})}{2}\sin 2\beta - I_{uv}]p' + [\frac{(1+\sigma_{12})}{2} - \frac{(1-\sigma_{12})}{2}\cos 2\beta + I_{vv}]q'$$

$$-I_{vz}(r'+\beta'') = [\frac{(1-\sigma_{12})}{2}\cos 2\beta + I'_{uv}]p\beta' + [-I'_{vv} - (1-\sigma_{12})\sin 2\beta]q\beta' \quad \text{(A26)}$$

$$+ I'_{vz}(r+\beta')\beta' + p\bar{H}_z - (r+\beta')\bar{H}_u + \bar{M}_v$$

$$-I_{uz}p' - I_{vz}q' + (\sigma_1 + I_{zz})r' + I_{zz}\beta'' = I'_{uz}p\beta' + I'_{vz}q\beta'$$

$$\text{(A27)}$$

$$- I_{zz}(r+\beta')\beta' + q\bar{H}_u - p\bar{H}_v + \bar{M}_z$$

$$-\bar{b}kp' + (1+\bar{\delta}k\cos(\beta-\nu))r' + \beta'' = -\eta\beta' - \bar{g}\,k\sin\theta\cos(\psi+\beta)$$

$$+ (\bar{I}_{uu} - \bar{I}_{vv} - \bar{I}'_{uv})pq - \bar{b}k\,q(r+\beta') \quad \text{(A28)}$$

$$+ \bar{I}'_{zz}(p^2+r^2)$$

where $\bar{H}_\alpha = \dfrac{H_\alpha}{A\Omega}$

$$\bar{M}_\alpha = \frac{M_\alpha}{A\Omega^2}$$

$$I'_{\alpha\omega} = \frac{\partial I_{\alpha\omega}}{\partial\beta}$$

Some of the terms in (A28) have been simplified by substituting for the $I_{\alpha\omega}$ their values given in Appendix B.

The relationship between the Euler angle rates and p, q, r is

$$
\begin{aligned}
p &= \acute{\theta}\cos(\psi+\beta) + \acute{\phi}\sin\theta\sin(\psi+\beta) \\
q &= -\acute{\theta}\sin(\psi+\beta) + \acute{\phi}\sin\theta\cos(\psi+\beta) \qquad \text{(A29)} \\
r &= \acute{\psi} + \acute{\phi}\cos\theta
\end{aligned}
$$

Appendix B

Moments of Inertia

$$I^*_{uu} = m[\frac{(1-\sin\gamma)}{\gamma}\frac{R^2}{2} + h^2 + \delta^2 \sin^2(\beta-\nu)]$$

$$I^*_{vv} = m[(\frac{(1+\sin\gamma)}{\gamma}\frac{R^2}{2} + h^2 + 2\delta R\ k\ \cos(\beta-\nu) + \delta^2\cos^2(\beta-\nu)]$$

$$I^*_{zz} = m[R^2 + 2\delta R\ k\ \cos(\beta-\nu) + \delta^2]$$

$$I^*_{uv} = -m\delta\sin(\beta-\nu)[R\,k + \delta\cos(\beta-\nu)]$$

$$I^*_{uz} = mh[R\,k + \delta\cos(\beta-\nu)]$$

$$I^*_{vz} = -m\,h\,\delta\sin(\beta-\nu)$$

$$\bar{I}_{uu} = (1-\frac{\sin\gamma}{\gamma})/2 + b^2 + \bar{\delta}^2\sin(\beta-\nu)$$

$$\bar{I}_{vv} = (1+\frac{\sin\gamma}{\gamma})/2 + b^2 + 2\bar{\delta}k\ \cos(\beta-\nu) + \bar{\delta}^2\cos^2(\beta-\nu)$$

$$\bar{I}_{zz} = 1 + 2\bar{\delta}k\ \cos(\beta-\nu) + \bar{\delta}^2$$

$$\bar{I}_{uv} = -\bar{\delta}\sin(\beta-\nu)[k + \bar{\delta}\cos(\beta-\nu)]$$

$$\bar{I}_{uz} = b[k + \bar{\delta}\cos(\beta-\nu)]$$

$$\bar{I}_{vz} = -b\bar{\delta}\sin(\beta-\nu)$$

$$I_{\alpha\beta} = \epsilon\bar{\gamma}\ \bar{I}_{\alpha\beta}$$

$$\bar{I}'_{uu} = \bar{\delta}^2 \sin 2(\beta-\nu)$$

$$\bar{I}'_{vv} = -2\bar{\delta}k \sin(\beta-\nu) - \bar{\delta}^2 \sin 2(\beta-\nu)$$

$$\bar{I}'_{zz} = -2\bar{\delta}k \sin(\beta-\nu)$$

$$\bar{I}'_{uv} = -k\bar{\delta}\cos(\beta-\nu) - \bar{\delta}^2 \cos 2(\beta-\nu)$$

$$\bar{I}'_{uz} = -b\bar{\delta}\sin(\beta-\nu)$$

$$\bar{I}'_{vz} = -b\bar{\delta}\cos(\beta-\nu)$$

$$I'_{\alpha\beta} = \epsilon\bar{\gamma}\, \bar{I}'_{\alpha\beta}$$